ANL-7968
LMFBR Fuel Recycle
(UC-79c)

ARGONNE NATIONAL LABORATORY
9700 South Cass Avenue
Argonne, Illinois 60439

DEVELOPMENT AND PERFORMANCE OF A HIGH-SPEED, LONG-ROTOR CENTRIFUGAL CONTACTOR FOR APPLICATION TO REPROCESSING LMFBR FUELS

by

G. J. Bernstein, D. E. Grosvenor,
J. F. Lenc, and N. M. Levitz

Chemical Engineering Division

NOTICE

This report was prepared as an account of work sponsored by the United States Government. Neither the United States nor the United States Atomic Energy Commission, nor any of their employees, nor any of their contractors, subcontractors, or their employees, makes any warranty, express or implied, or assumes any legal liability or responsibility for the accuracy, completeness or usefulness of any information, apparatus, product or process disclosed, or represents that its use would not infringe privately owned rights.

January 1973

MASTER

DISCLAIMER

This report was prepared as an account of work sponsored by an agency of the United States Government. Neither the United States Government nor any agency Thereof, nor any of their employees, makes any warranty, express or implied, or assumes any legal liability or responsibility for the accuracy, completeness, or usefulness of any information, apparatus, product, or process disclosed, or represents that its use would not infringe privately owned rights. Reference herein to any specific commercial product, process, or service by trade name, trademark, manufacturer, or otherwise does not necessarily constitute or imply its endorsement, recommendation, or favoring by the United States Government or any agency thereof. The views and opinions of authors expressed herein do not necessarily state or reflect those of the United States Government or any agency thereof.

DISCLAIMER

Portions of this document may be illegible in electronic image products. Images are produced from the best available original document.

TABLE OF CONTENTS

	Page
ABSTRACT	7
I. INTRODUCTION	7
II. RELATIONSHIP OF THE DESIGN AND OPERATING CONDITIONS TO THE PERFORMANCE OF SR-TYPE CENTRIFUGAL CONTACTORS	8
III. DESIGN, FABRICATION, AND TESTING OF CONTACTOR	14
IV. TEST FACILITY	15
V. PERFORMANCE TESTS	24
A. Separating Capacity and Hydraulic Characteristics	24
B. Effect of Solids on Contactor Operation	29
C. Determination of Extraction Efficiency	32
VI. DISCUSSION AND CONCLUSIONS	34
APPENDIX A. NUCLEAR CRITICALITY	36
APPENDIX B. CRITICAL SPEED CALCULATIONS FOR ROTOR ASSEMBLY	38
APPENDIX C. CALCULATION OF AIR-WEIR PRESSURES	42
APPENDIX D. ROTOR PUMPING CAPACITY	47
ACKNOWLEDGMENTS	51
REFERENCES	52

LIST OF FIGURES

No.	Title	Page
1	ANL Contactor (SR Mixing Mode)	9
2	Separating Capacities of Centrifugal Contactors.	11
3	Isometric View of Air-Controlled Weir.	13
4	Rotor and Removable Mixing Paddle.	16
5	Draw Bar and Rotary Air Seal	16
6	Spindle and Mounting Plate	17
7	Centrifugal Contactor Assembly	18
8	Schematic Layout of Contactor Test Facility.	18
9	Centrifugal Contactor Test Facility.	20
10	Centrifugal Contactor.	21
11	Motor Drive for Centrifugal Contactor.	22
12	Rotor Speed Pickup	23
13	Circuitry for Measurement of Rotor	23
14	Separating Capacity of Centrifugal Contactor with 4-in.-dia Rotor. Organic phase: 15% TBP in Ultrasene. Aqueous phase: 0.5M HNO_3. <1% entrainment.	25
15	Separating Capacity of Centrifugal Contactor with 4-in.-dia Rotor. Organic phase: 30% TBP in Ultrasene. Aqueous phase: 0.5M HNO_3. <1% entrainment.	25
16	Separating Capacity of Centrifugal Contactor with 4-in.-dia Rotor. Organic phase: 15% TBP in n-dodecane. Aqueous phase: 0.5M HNO_3. 1% entrainment..	27
17	Separating Capacity of Centrifugal Contactor with 4-in.-dia Rotor. Organic phase: 30% TBP in n-dodecane. Aqueous phase: 0.5M HNO_3. 1% entrainment..	27
18	Dual-Purpose Centrifuge Tube	28
19	Mixing Paddles Tested in Centrifugal Contactor Runs. . .	30
20	Schematic Drawing of Rotor and Shaft Assembly.	39
21	Static Deflection of Rotor as a Function of Bowl Length.	39

LIST OF FIGURES (Cont'd)

No.	Title	Page
22	Interface Control Weirs of Centrifugal Contactor	43
23	Air-Weir Pressure as a Function of Total Throughput. Curve A, 1% Aqueous Phase in Organic Effluent and <1 vol % Organic in Aqueous Effluent. Curve B, 1% Organic Phase in Aqueous Effluent and <1 vol % Aqueous in Organic Effluent. Point C, 1% Aqueous in Organic Effluent and 1 vol % Organic in Aqueous Effluent	46
24	Hydraulic Head Developed in a Rotor.	49

LIST OF TABLES

No.	Title	Page
1	Summary of Contactor Runs with MnO_2 Solids (SR Mixing Mode).	32
2	Stage Efficiencies for Uranium Extraction. Run UXS-1.	33
3	Calculated and Experimental Air-Weir Pressures	45

DEVELOPMENT AND PERFORMANCE OF A HIGH-SPEED, LONG-ROTOR CENTRIFUGAL CONTACTOR FOR APPLICATION TO REPROCESSING LMFBR FUELS

by

G. J. Bernstein, D. E. Grosvenor, J. F. Lenc, and N. M. Levitz

ABSTRACT

A centrifugal contactor with a high length-to-diameter rotor has been developed and successfully tested. It is designed to be dimensionally safe for nuclear criticality when solutions having high concentrations of plutonium are processed in it. Mechanical and hydraulic performance was excellent. By close attention to critical-speed considerations during design and careful fabrication to the required tolerances, essentially all vibrations in the high-speed rotor were eliminated. By proper selection of mixing paddle size and mixing chamber dimensions, problems in flow surging were eliminated.

Extraction tests were made with uranyl nitrate and 30% tributyl phosphate in n-dodecane. Essentially 100% stage efficiency was achieved readily. A bank of contactors of the size tested could easily process 1 tonne/day of mixed uranium-plutonium reactor fuel or plutonium alone.

In tests to evaluate any effects on contactor operability of finely divided solids in the feed solutions, no operating difficulties were encountered.

I. INTRODUCTION

Solvent extraction processes are currently being used to separate uranium and plutonium from each other and from fission products in irradiated uranium or uranium-plutonium fuel. Several solvent extraction cycles are necessary to achieve the required degree of purification of the actinides. Adaptation of solvent extraction processes such as the Purex process to the recovery of plutonium from fast breeder reactor fuels will require the development of advanced technology. In the Purex process, the solvent (organic phase) is tributyl phosphate in a kerosene-type diluent, and the aqueous phases contain nitric acid. In application of the Purex process at the AEC's Savannah River (SR) plant to the first cycle for production-reactor fuels, centrifugal contactors are being used at throughputs of 40-60 gpm.[1] These units have settling zones 10 in. in diameter and about 14 in. long. Considering as a basis a 5 tonne/day plant, a bank of such high capacity contactors is expected to be suitable for Purex-type first cycle extraction of low-plutonium, light-water reactor (LWR) fuel, or high-plutonium, short-cooled Liquid Metal Fast Breeder Reactor (LMFBR) fuel[2] if the feed is dilute and contains soluble nuclear poisons. These large centrifugal contactors would not

be critically safe for processing solutions containing high concentrations of plutonium. The operation could be accomplished better in centrifugal contactors having a critically favorable geometry. Additional advantages of centrifugal contactors over extraction columns or mixer-settlers (that have been demonstrated at SR) are reduced radiation damage to the solvent and quick flushout of equipment at the end of a processing campaign.

A program was undertaken to extend the centrifugal contactor design developed at the Savannah River Laboratory[3-7] to a configuration suitable for efficient handling of plutonium-bearing streams in the solvent-extraction processing of LMFBR fuels. Principal objectives were to ensure nuclear safety by limiting the diameter of the unit to a critically favorable dimension and to maintain a relatively high capacity by increasing the bowl length and operating speed. This report describes the design, development, and testing of a small-diameter, paddle-mixer type (SR) contactor. In a companion report,[8] the development of a novel annular-mixer centrifugal contactor is described.

II. RELATIONSHIP OF THE DESIGN AND OPERATING CONDITIONS TO THE PERFORMANCE OF SR-TYPE CENTRIFUGAL CONTACTORS

A centrifugal contactor for a solvent extraction process performs two principal functions: (1) vigorous mixing of aqueous and organic phases to effect the transfer of a solute from one phase to the other and (2) separation of the mixed phases under centrifugal force to achieve a much more rapid separation than could be achieved by settling under the force of 1 gravity.

The ANL contactor (Fig. 1) comprises principally a fixed casing (or stator) inside which spins a 4-in.-ID rotor suspended from an overhead bearing support. The rotor is supported only at the top in order to avoid problems that might be caused by bottom bearings operating in corrosive solutions. The spindle assembly* that supports the rotor accommodates a 1 1/4-in.-dia shaft and is suitable for operation at speeds up to 4000 rpm. Beneath the rotor is a mixing chamber into which aqueous and organic process solutions are fed from inlets at the bottom of the contactor. Attached to the bottom of the shaft that supports the rotor is a paddle that mixes the two phases in the mixing chamber. The mixture from the mixing chamber enters an opening in the bottom of the rotor, and the organic and aqueous phases are separated by centrifugal force as they flow up through the rotor. The separated phases are discharged from the top of the rotor into different collecting rings.

Since, in Purex processes, the phases are relatively easy to mix, the phase-separating effectiveness of a contactor is a more critical criterion in these processes than is mixing effectiveness. Capacity is much more likely to be limited by separating capacity, although extremely vigorous mixing can have a deleterious effect on separating capacity if certain kinds of emulsions form.

---

*Model No. 4000 F-1-M, Russel T. Gilman, Inc., Grafton, Wisconsin.

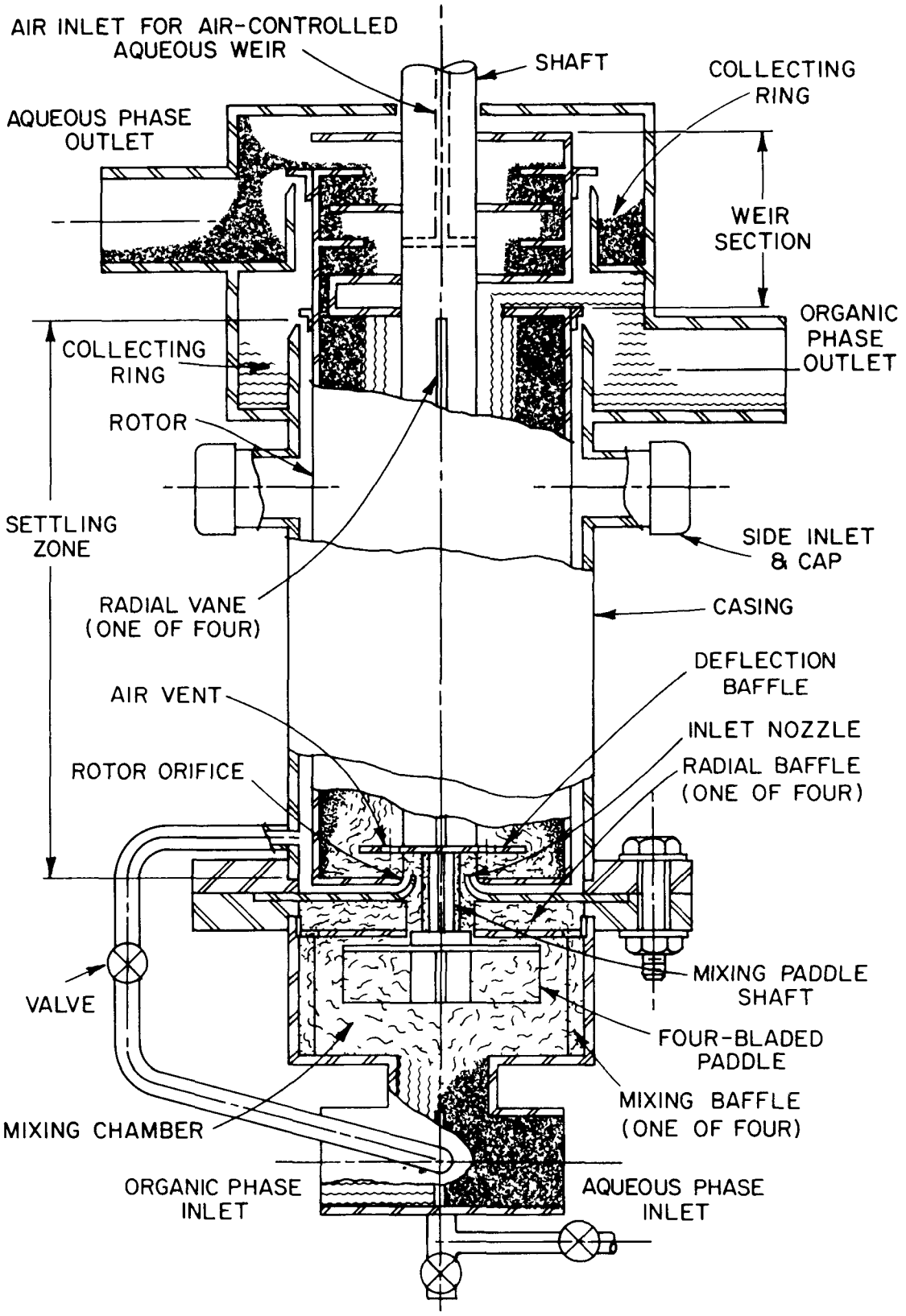

FIG. 1. ANL Contactor (SR Mode)

At the outset of the program, available data on the performance of centrifugal contactors of the SR type were evaluated. An expression developed at ANL for estimating the separating capacity was in the form

$$q_s \propto \frac{N_c^2 D_b^3 L}{10^5 N_m D_m} \qquad (1)$$

where q_s = separating capacity, gpm
N_c = rotor speed, rpm
D_b = rotor ID, in.
L = settling length of rotor, in.
N_m = mixing paddle speed, rpm
D_m = mixing paddle diameter, in.

Since the rotor and mixing paddle are on the same shaft in the ANL contactor, $N_c = N_m$.

Figure 2 shows separating capacities of several centrifugal contactors plotted against the value of the above expression. The SR units[4,5,7] for which separating capacities are plotted are those studied at Savannah River; the WAK unit[9] is a design developed from the SR design and studied in West Germany. The 4-in.-dia unit is the ANL stainless steel contactor described in this report. For given values of the expression, the measured values of the separating capacities fall within a band in which the high value is about twice the low value.

Examination of equation 1 reveals clearly that the diameter of the rotor has a much greater influence on separating capacity than do the settling length of the rotor, the rotor speed, and the mixing paddle diameter. Consequently, for high separating capacity, the rotor of a contactor should have the maximum diameter that is critically safe.

The plutonium concentration in Purex-type process flowsheets for which this type of contactor may be employed is not expected to exceed 200 g/liter. The maximum acceptable inside diameter of the casing was determined by treating the contactor assembly as an infinite cylinder. On the basis of data[10] on safe diameters of infinite water-reflected cylinders of $Pu(NO_3)_3$ solutions, a stator ID of 5.4 in. was determined to be critically safe for plutonium concentrations as high as 200 g/liter. An ID of 4.75 in. for the stator (in the unit shown in Fig. 1) and a rotor OD of 4.2 in. were selected.

The collecting rings surrounding the inner section at the top of the contactor had ID's of 7 in. These were larger than needed, to permit the rotor to be tested at maximum separating capacity without the risk of flow rates being limited by the flow capacity of the rings and discharge lines. On the basis of operating experience with the experimental unit (discussed below), it is believed that the ID of the collecting region can be reduced to less than 5.4 in. without significantly affecting separating capacity. A more detailed treatment of the effect of criticality on design appears in Appendix A.

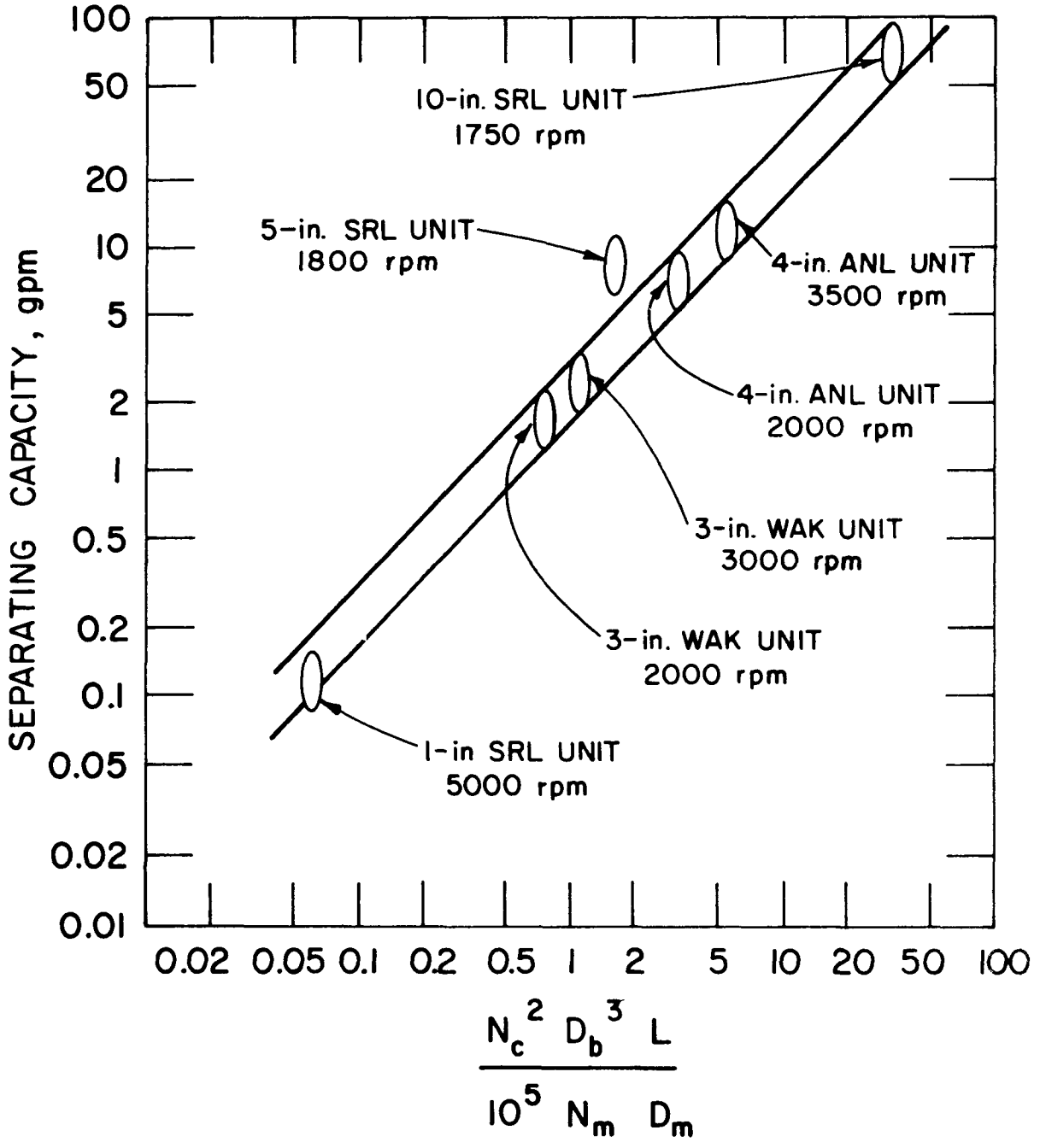

FIG. 2. Separating Capacities of Centrifugal Contactors

The length of the rotor and its operating speed are limited by the critical speed of the shaft and rotor assembly. At the critical speed, any vibration resulting from rotor imbalance is strongly reinforced and can lead to excessive deflection, high stresses, and possible failure of the equipment. Because the ANL contactor has a long rotor, its critical speed is of much greater significance to its design than is the critical speed of the rotor for the SR contactor. An indication of the relative significance can be found by use of a general equation for determining the critical speed of a steel shaft of uniform diameter.[11]

$$N_{cs} = \frac{795{,}196\ d^2}{(WL_s^{\ 3})^{1/2}} \qquad (2)$$

where N_{cs} = critical speed, rpm
d = shaft diameter, in.
L_s = shaft length, in.
W = shaft weight, lb.

For the ANL small-diameter rotor with a central shaft, the weight is about 1 lb/in. so that numerically, L_s was equal to W. Consequently, Eq. 2 reduces to

$$N_{cs} \propto \frac{1}{L_s^{\ 2}} \qquad (3)$$

It is therefore clear that if the length and speed of the rotor are increased to obtain high throughput, extreme care must be taken in the design and fabrication of the rotor so that the rotor can safely operate at speeds close to its critical speed.

Calculations of critical speeds for the entire rotor assembly (see Appendix B) indicated that the rotor assembly, which is 15 in. long, would have a first critical speed of about 5400 rpm. Since the operating speed generally recommended as safe for rotating bodies is about 70% of the critical speed, operating speeds up to about 3500 rpm would be permissible with such a rotor. In the ANL unit, the weir section occupies the upper 3 in. of the bowl length; the remaining 12 in. is available for use as a settline zone. The length-to-diameter (L/D) ratio of 3 for the settling zone and the operating speed of 3500 rpm extended the study of operating characteristics beyond the range covered by the SR unit, which has a settling-zone L/D ratio of about 1.4 and an operating speed of 1750 rpm.

The baffled mixing chamber has a ∿4 1/2-in. ID and a ∿2-in. depth and can accommodate a variety of mixing paddles. With a paddle diameter of 3 1/4 in., a rotor ID of 4 in., and a rotor settling length of 12 in., equation 1 shows that the separating capacity of the contactor should be ∿7 gpm at 2000 rpm and ∿12 gpm at 3500 rpm. As shown in Fig. 2, the capacities found in the tests were very close to the predicted ranges.

The hydraulic performance of the contactor can be understood by reference to Fig. 1. Aqueous and organic streams are fed into the inlet tee below the mixing chamber. As they flow through the mixing chamber,

they are vigorously mixed by the paddle. The mixed phases are discharged through openings in the periphery of the mixing chamber into the zone above the chamber. Four fixed radial baffles direct the mixture to the nozzle; the mixture flows through the nozzle into the bottom orifice of the rotor.

The deflection baffle immediately above the orifice prevents the mixture from bypassing part of the settling zone, directing it to the outer regions of the rotor where centrifugal force is higher. Vent holes in the baffle permit entrained air to escape and flow upward through the space adjacent to the rotor shaft. Four vertical vanes in the rotor accelerate the mixture to rotor speed, and the phases are separated under centrifugal force (about 450 *g* at 3500 rpm) as they flow upward through the rotor. The heavy (aqueous) phase moves outward, displacing the light (organic) phase inward. The aqueous phase flows through a system of weirs to the upper discharge ports. The organic phase flows over an inner weir and is discharged through four passages built in the form of a hollow cross. Figure 3 is an isometric sketch of the weir system as used in the centrifugal contactor. (The sectional view of the weir elements as shown in Fig. 1 is a partial distortion since the passages shown do not lie in the same vertical plane.)

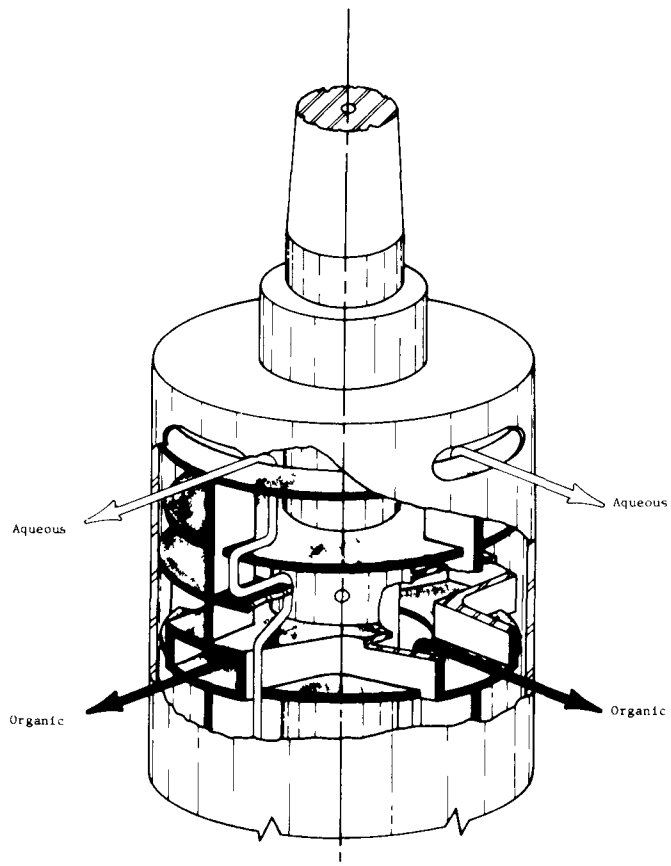

FIG. 3. Isometric View of Air-Controlled Weir

Any air that has become mixed with the two phases is discharged with the organic phase. The effluent streams are discharged into collecting rings where they continue to spin in the same direction as the rotor. These streams leave the rings through tangential outlet lines. When a number of contactors are arranged for countercurrent solvent extraction, the effluent streams become inlet streams for adjacent contactors.

In the upper portion of the rotor settling zone, the aqueous and organic phases are separated except for a band of emulsion that floats between them; this emulsion band corresponds to the interface conventional in other types of contactors. The width of this emulsion band increases as the flow rate through the rotor increases. If the separating capacity of the unit is exceeded, some of the unseparated emulsion may extend inward and flow out with the organic phase, or it may extend outward and flow out with the aqueous phase. The position of the emulsion band can be shifted by applying air pressure to the aqueous-phase weir system discussed in the following paragraph. However, ultimately, as flow rates are increased, the emulsion band becomes so wide that some of it flows out with both effluent streams. The contactor is arbitarily said to be operating at its maximum separating capacity when contamination of each effluent stream by the other reaches 1%.

The air-controlled weir system was developed at Savannah River.[6] This system makes the rotor suitable for operation with a broader range of phase densities and aqueous-to-organic (A/O) flow ratios than could be accommodated with a fixed set of weirs alone. The organic phase flows over the lower weir and through the arms of the hollow cross. The aqueous phase flows around an underflow baffle between the arms of the cross and then over-and-under its weirs. The topmost aqueous weir serves to prevent blowout of the control air. Air pressure applied through the hollow rotor shaft imposes a resistance to the flow of aqueous phase over the lower aqueous weir. The combined air pressure and aqueous-phase back pressure balances the combined aqueous and organic pressure developed in the settling zone below the bottom weir.

The position of the unseparated emulsion can be shifted by adjustment of the weir air pressure. Thus, to move the emulsion band inward (in order to reduce contamination of the aqueous effluent stream), the air pressure is increased to increase the overall effective back pressure applied to the aqueous phase. This system offers a high degree of control. The calculations used in determining the anticipated air control pressures are given in Appendix C.

III. DESIGN, FABRICATION, AND TESTING OF CONTACTOR

The centrifugal contactor was fabricated from Types 304 and 304L stainless steel. Machining tolerances were generally held to ±1 mil in order to maintain uniform weight distribution and to hold the alignment of the rotor axis within the 3 mils maximum allowable run-out based on the critical speed analysis. For weld areas that could be reached readily, welding was done by the tungsten-inert gas (TIG) technique. Those regions for which the weld area was not accessible (e.g., the weir zone) were

welded by the electron beam (EB) technique. The final alignment of the rotor in the spindle was done by precision-grinding the Morse taper on the completed rotor to fit the taper of the spindle. The complete rotor is shown in Fig. 4. (The removable mixing paddle shown at the left is designed so that the paddle and the extension shaft on which it is mounted can be removed. This design feature permits the rotor to be used in the contactor when it is modified for annular mixing as described in a companion topical report.[8] The ring on the paddle (Fig. 4) was included in the original design to improve dynamic stability. Performance of the rotor during subsequent testing showed that this stabilizing ring was not needed.)

The rotor is held in the spindle taper bore by means of a draw rod that passes through the hollow spindle shaft and screws into the top of the rotor shaft. Figure 5 shows the draw rod and rotary air seal.* The spindle itself is bolted to a heavy steel mounting plate and is also surrounded by a retaining sleeve to prevent deflection during operation. Figure 6 shows the spindle mounting plate and the rotary air seal (through which air pressure is applied to the aqueous weir). The small tapered hole in the front of the spindle support (Fig. 6) is used as an inlet for an air purge. This purge protects the spindle bearing from any solvent or acid fumes that might bypass a protective seal installed on the bottom of the mounting plate.

Dynamic testing of the completed rotor was carried out with a Vibrapac II** vibration analyzer, which indicates vibration displacement in mils. Tests with the rotor running empty at 3500 rpm showed that displacements were 0.040 mil (measured at the top of the rotor support spindle) and 0.008 mil (measured at the bottom of the spindle). These values are considered very low. Subsequent vibration tests made with liquid running through the contactor showed even lower displacements than were measured in the dry tests. Figure 7 shows the completed contactor as it would appear when assembled on its mounting plate.

The fabrication drawings for the contactor were prepared by the Chemical Engineering Division drafting group (part of the ANL Central Shops Division) under the general drawing number CE-6490.

IV. TEST FACILITY

A special test facility was constructed to permit testing of the centrifugal contactor with various aqueous and organic solutions and ultimately with natural uranium. Figure 8 is a schematic layout of the components of the test facility. Aqueous and organic feed solutions are prepared and held in the large supply tanks located on the floor. The solutions are pumped into the elevated tanks located on an overhead platform. The discharge ends of the pump lines are equipped with stainless steel wire wool filters to remove extraneous solids. Solutions flow from the tanks through control valves and rotameters into the contactor. Each overhead tank is equipped with a removable overflow standpipe. During runs to test separating capacity, a short standpipe is used so that any

---

*Model 1105, Manufactured by Deublin Co., Northbrook, Ill.
**Balance Technology, Inc., Ann Arbor, Mich.

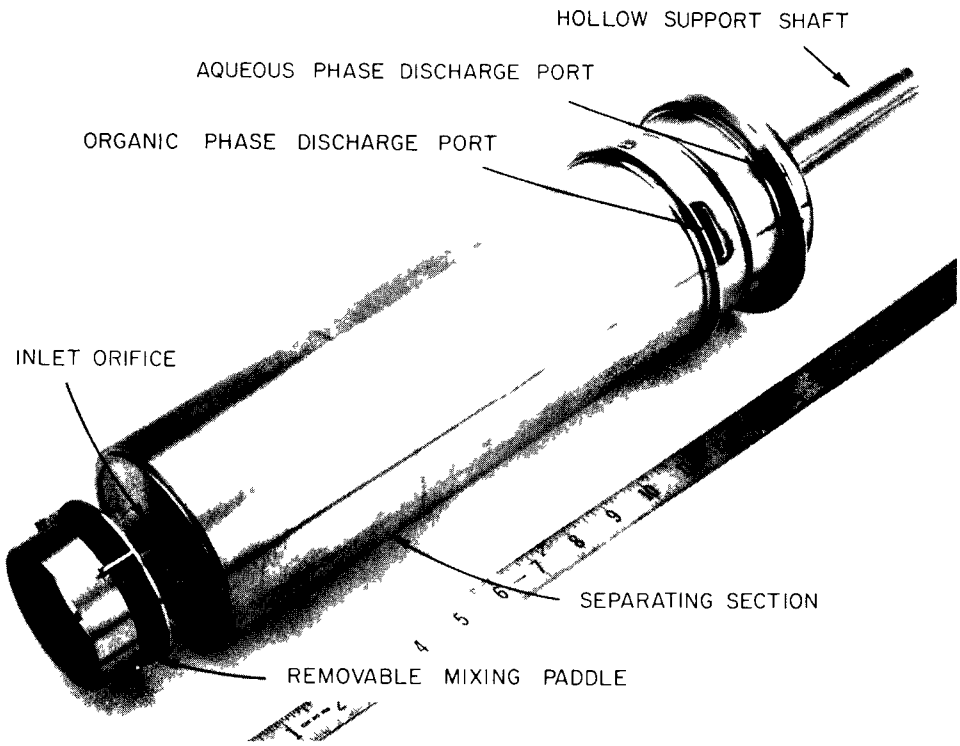

FIG. 4. Rotor and Removable Mixing Paddle (ANL Neg. No. 308-2354A)

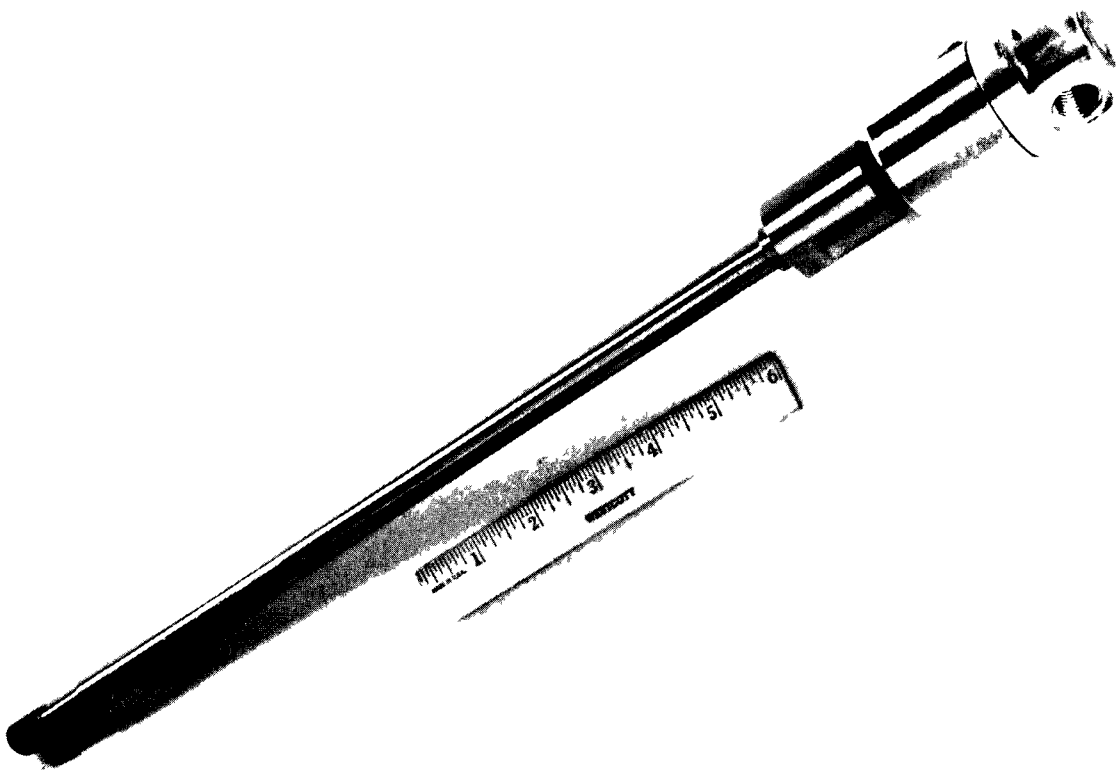

FIG. 5. Draw Bar and Rotary Air Seal (ANL Neg. No. 308-2370)

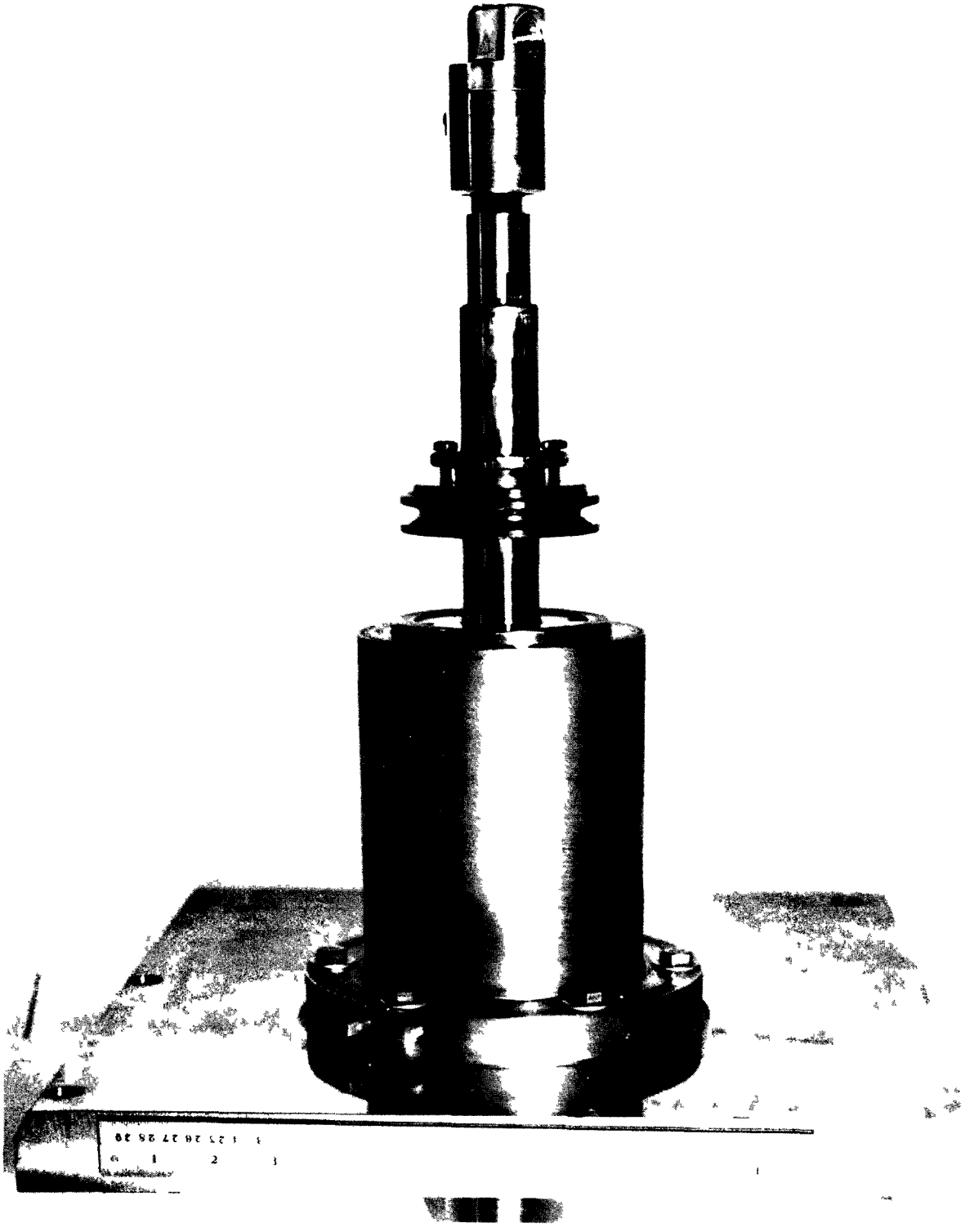

FIG. 6. Spindle and Mounting Plate (ANL Neg. No. 308-2367)

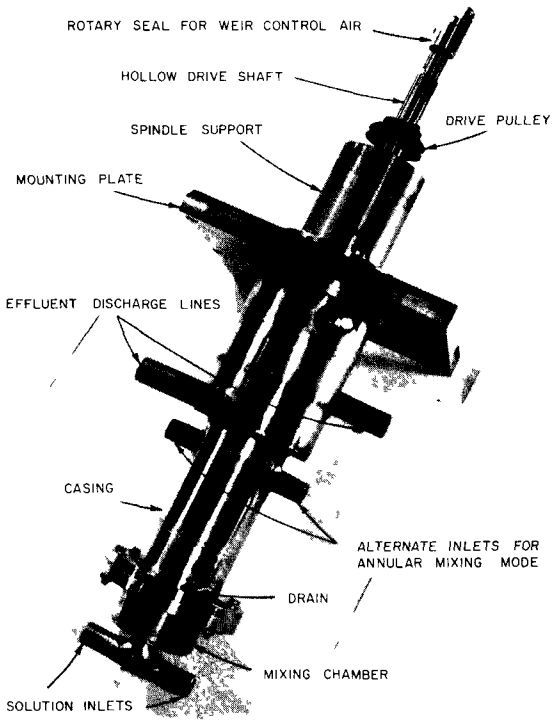

FIG. 7

Centrifugal Contactor Assembly
(ANL Neg. No. 308-2361A)

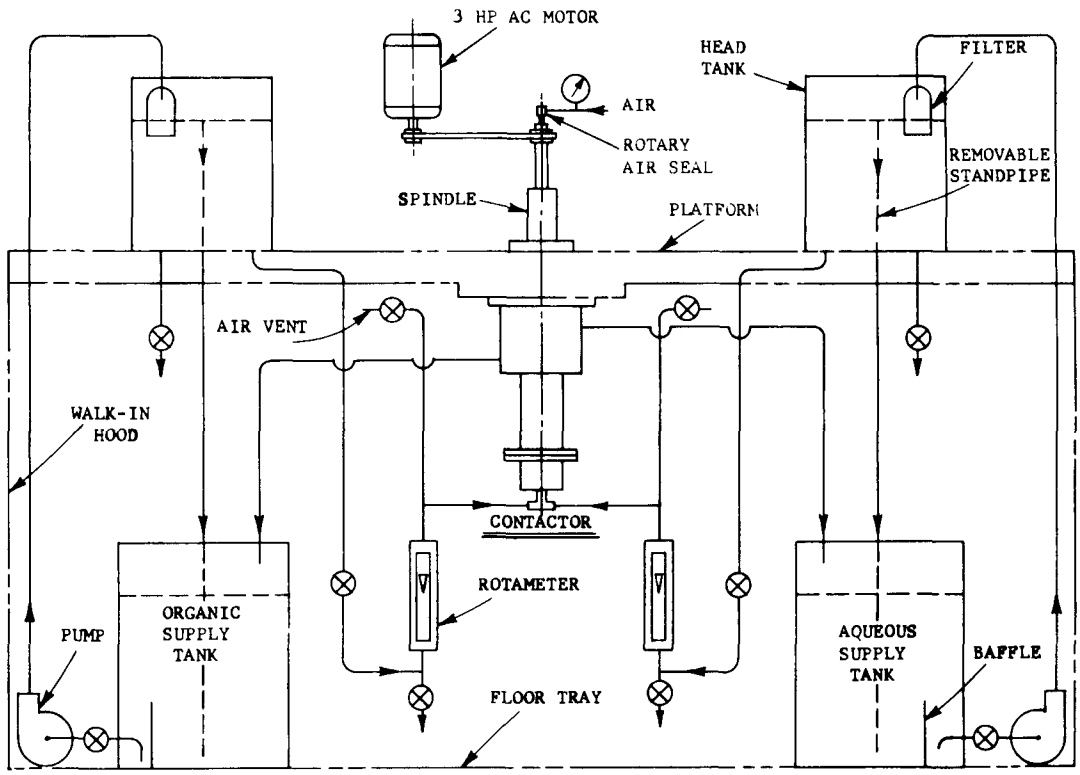

FIG. 8. Schematic Layout of Contactor Test Facility

excess solution pumped to the overhead tank is returned to the supply tank while a constant head is maintained for flow through the rotameter. During uranium extraction runs (see Section V.C), a tall standpipe was installed in each overhead tank so the tank could be filled nearly to the top; the pump was then shut down, and the overhead tank served as a supply tank and the floor supply tank as a receiver. The area below the platform (Fig. 8) is enclosed in a ventilated hood to confine any vapors from process solutions. (As shown in Fig. 8, the aqueous and organic inlet lines are each on the same side of the contactor as the respective outlet lines. This arrangement was used so that the effluent streams could be recirculated to the supply tanks by the most direct route. In an array of contactors arranged for countercurrent extraction, the inlet and outlet connections for a phase would be on opposite sides of each contactor as shown in Fig. 1.)

Figure 9 is a photograph of the contactor mounted in the test facility. One of the feed supply tanks is shown at the lower left corner. The overhead tank is on a platform above the contactor mounting plate. Feed solution runs through the rotameter shown below the contactor, and the flow rate is adjusted by the ball valve in the feed line. Figure 10 is a closeup view of the same contactor. The casing has been modified by cutting it and installing bolted flanges. This change was made to permit the contactor to be used for studies of the annular mixing mode, described in a companion report.[8] The heavy mounting plate and the rigid support minimize vibration when the rotor is operated at high speed. The rotor is belt-driven by a 3-hp ac induction motor mounted on the wall above the platform. Figure 11 shows the motor drive assembly, as well as the pressure gage for reading air pressure on the aqueous weir. The motor speed is controlled by a Varidyne* variable-frequency generator, and the rotor can be driven at speeds of 1200 to 3600 rpm. The drive system has worked very successfully in maintaining the desired rotor speeds while flow rates were varied.

The rotor speed is measured by means of a reed switch using appropriate circuitry to convert rpm into counts per minute (cpm). A permanent magnet (in the form of three small bar magnets) was cemented to the spindle shaft, and a small reed switch was mounted near the magnet as shown in Fig. 12. Each time the magnet passed the reed switch, the switch was actuated, producing a pulse for each revolution of the shaft. By the use of a diode pump, a current was generated that was proportional to the number of pulses. A microammeter calibrated to read rpm directly was used to indicate the rotor speed continuously. An impulse counter (maximum rate, 100 counts per second) was also built into the circuit for use when more accurate readings were desired. It gives a direct reading of revolutions over a 1-min timed interval. The system circuitry is shown in Fig. 13.

---

*Manufactured by U. S. Electrical Motors Div., Emerson Electric Co., Milford, Conn.

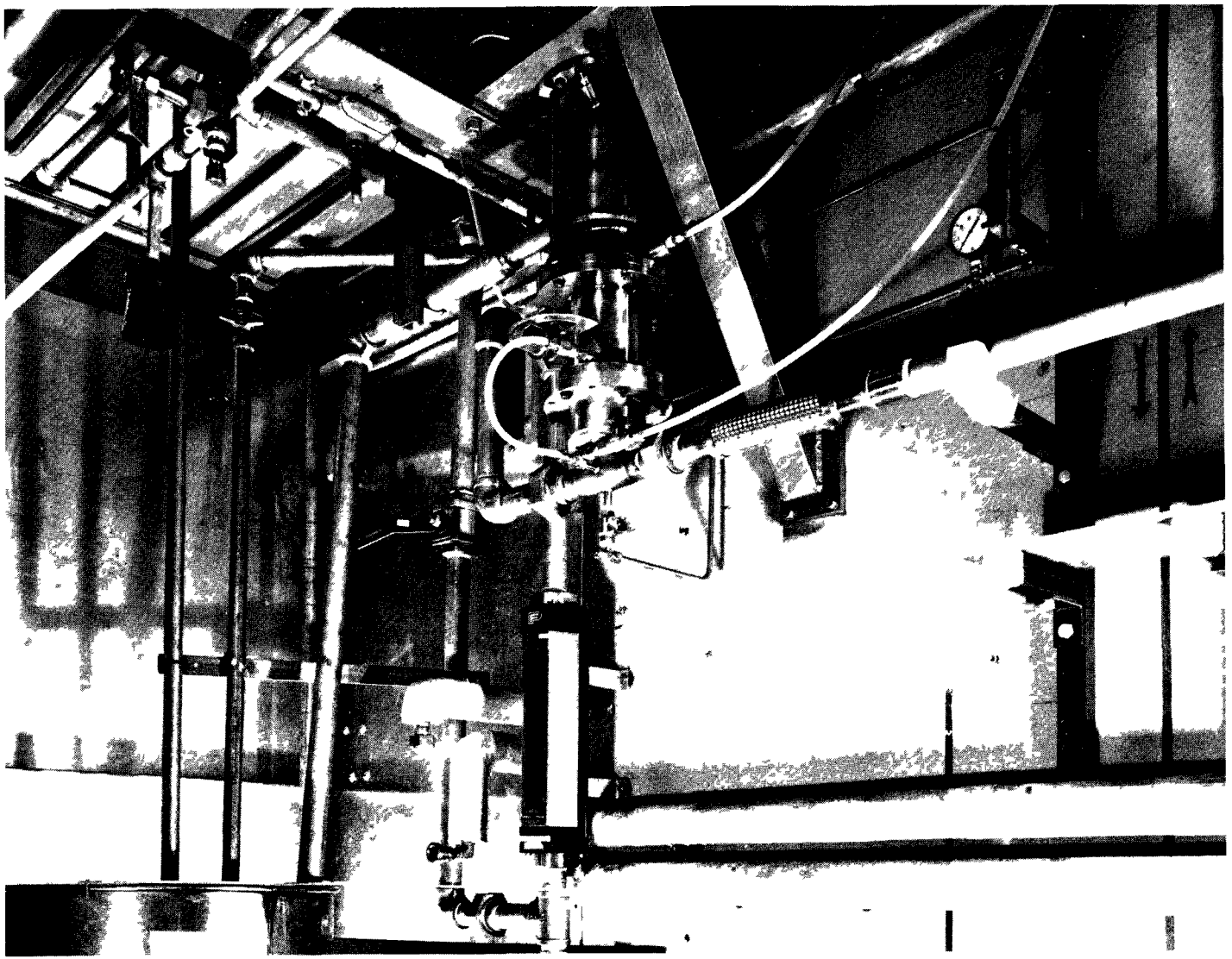

FIG. 9. Centrifugal Contactor Test Facility (ANL Neg. No. 308-2820)

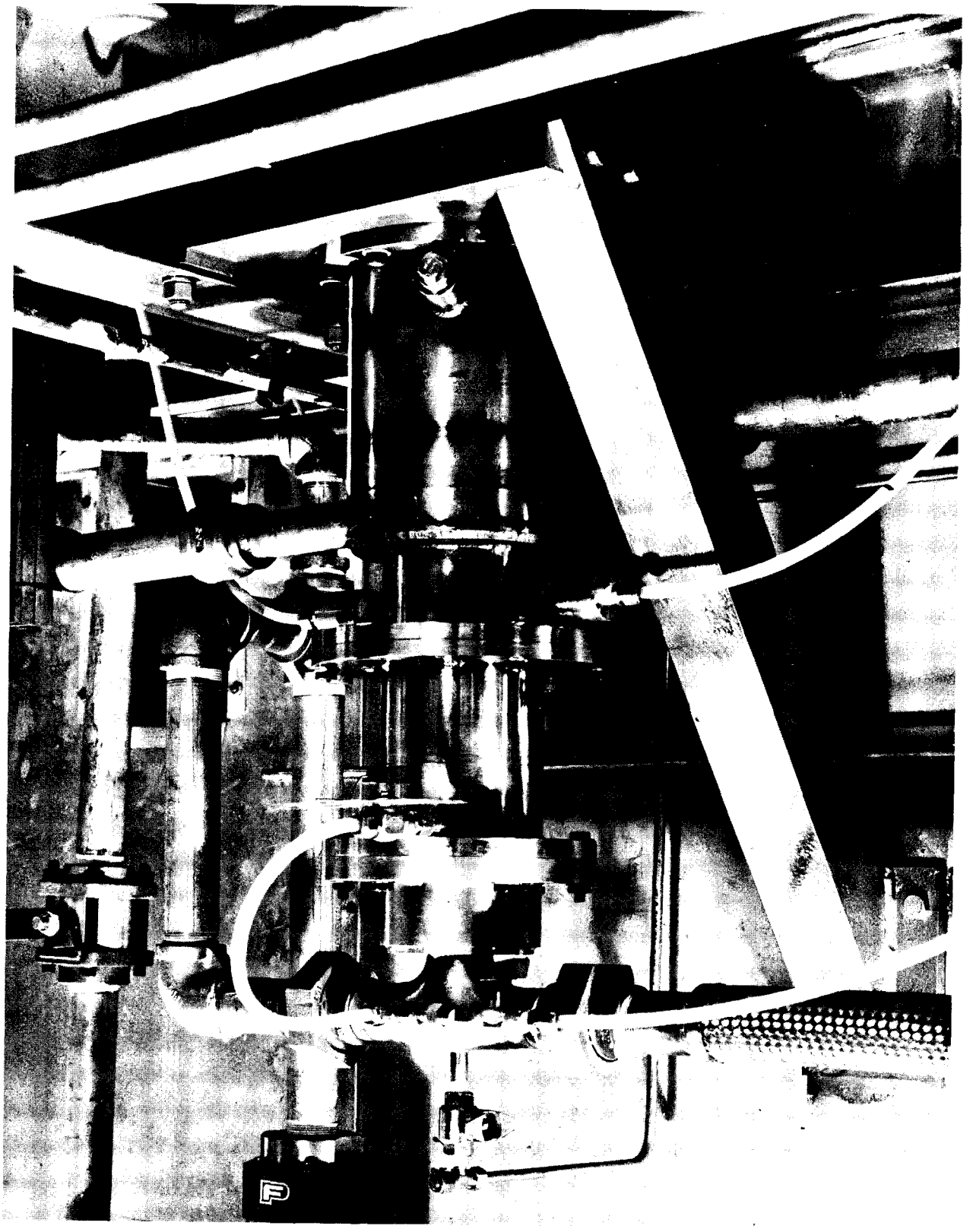

FIG. 10. Centrifugal Contactor (ANL Neg. No. 308-2821)

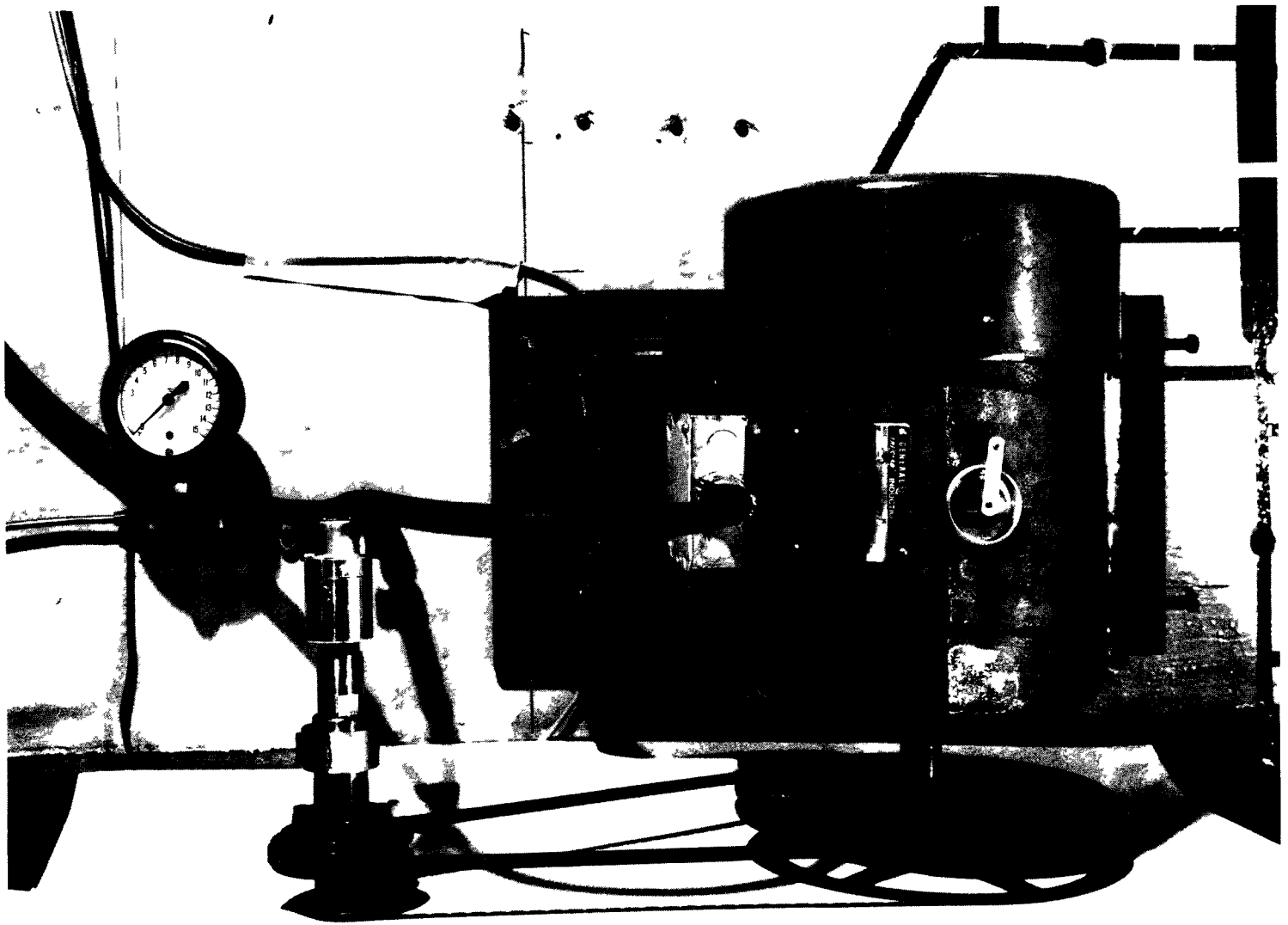

FIG. 11. Motor Drive for Centrifugal Contactor (ANL Neg. No. 308-2847)

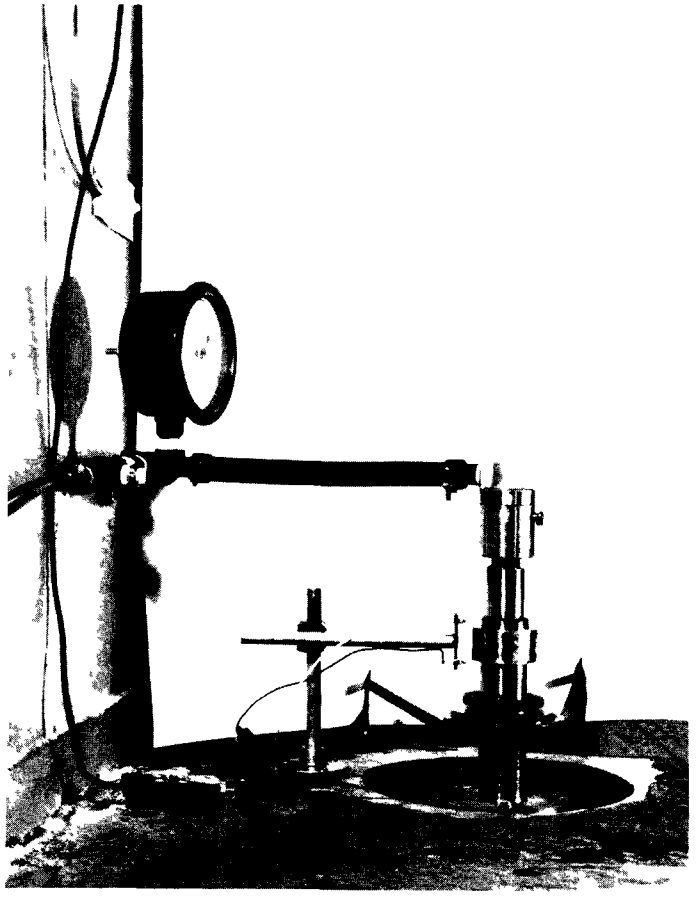

FIG. 12. Rotor Speed Pickup (ANL Neg. No. 308-2845)

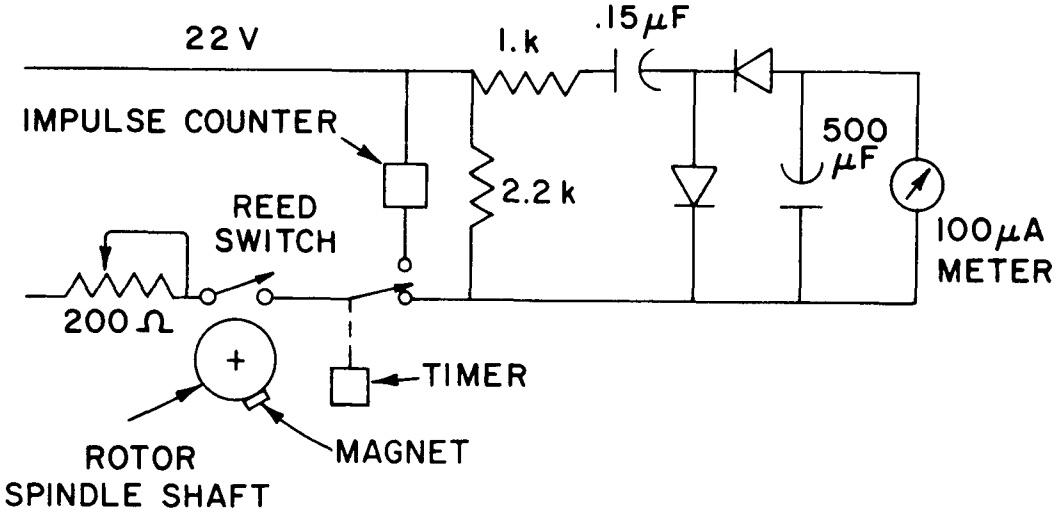

FIG. 13. Circuitry for Measurement of Rotor Speed

V. PERFORMANCE TESTS

A. Separating Capacity and Hydraulic Characteristics

The centrifugal contactor was tested under a variety of conditions involving different solution compositions, flow ratios, rotor speeds, and mixing paddle sizes to evaluate its separating capacity and hydraulic characteristics. Solutions employed for these tests were inactive, but simulated those generally associated with Purex solvent extraction processes. The initial tests were made with an aqueous phase of 0.5M HNO_3 and an organic phase of either 15 or 30% tributyl phosphate (TBP) in Ultrasene.* Separating capacity was measured over a range of rotor speeds of 2000 to 3500 rpm and for aqueous-to-organic (A/O) flow ratios of 0.33 to 4.0.

In tests with 15% TBP in Ultrasene, separating capacity of all rotor speeds tested was near the minimum value at A/O ratios of ∿2.0. At A/O ratios above and below ∿2.0, separating capacities were higher. At all A/O ratios, capacity increased with increasing rotor speed (Fig. 14). Capacities at an A/O of 0.5 ranged from about 6.8 gpm at 2000 rpm to about 11.4 gpm at 3500 rpm. At an A/O of 3, capacity was 9.2 gpm at 2000 rpm. At rotor speeds above 2000 rpm, throughput was found to be limited by the size of the inlet piping. The piping was subsequently enlarged for the tests with 30% TBP.

In the tests with 30% TBP in Ultrasene, minimum separating capacities over the range of speeds from 2000 to 3500 rpm were found at an A/O ratio of ∿1.0 (Fig. 15). Capacities as high as 17 gpm were attained at a rotor speed of 3500 rpm and an A/O ratio of 4. At low A/O ratios, the relative increase in capacity with increasing rotor speed was less than had been achieved with 15% TBP in Ultrasene.

During these tests, the air-controlled aqueous weir performed very satisfactorily in positioning the aqueous-organic emulsion (or interface) band between the organic and aqueous weirs at the top of the rotor (where the aqueous and organic phases are discharged). Air pressures used to achieve desired interface control ranged from 0 to 4 psig and conformed closely to values calculated with equations developed at Savannah River[6] (see Appendix C). The rotary seal gave excellent service over a period of more than 500 hr of operation with essentially no air leakage. The spindle also gave excellent service. Bearing temperatures were moderate (<50°C), even after extended periods of operation at high speed.

During the tests at higher A/O ratios in which high aqueous flow rates were employed, it was noted that contamination of the organic phase effluent stream reached 1%, while contamination of the aqueous phase effluent stream was below 1%, even though the air pressure on the aqueous weir had been reduced to zero. This suggests that better control could have been achieved under these conditions if the ID of the lower aqueous weir had been slightly larger. However, the present weir dimensions are suitable for Purex processing, in which A/O flow ratios greater than 2 are not likely to be encountered.

---

*A refined kerosene product of Atlantic Richfield Co.

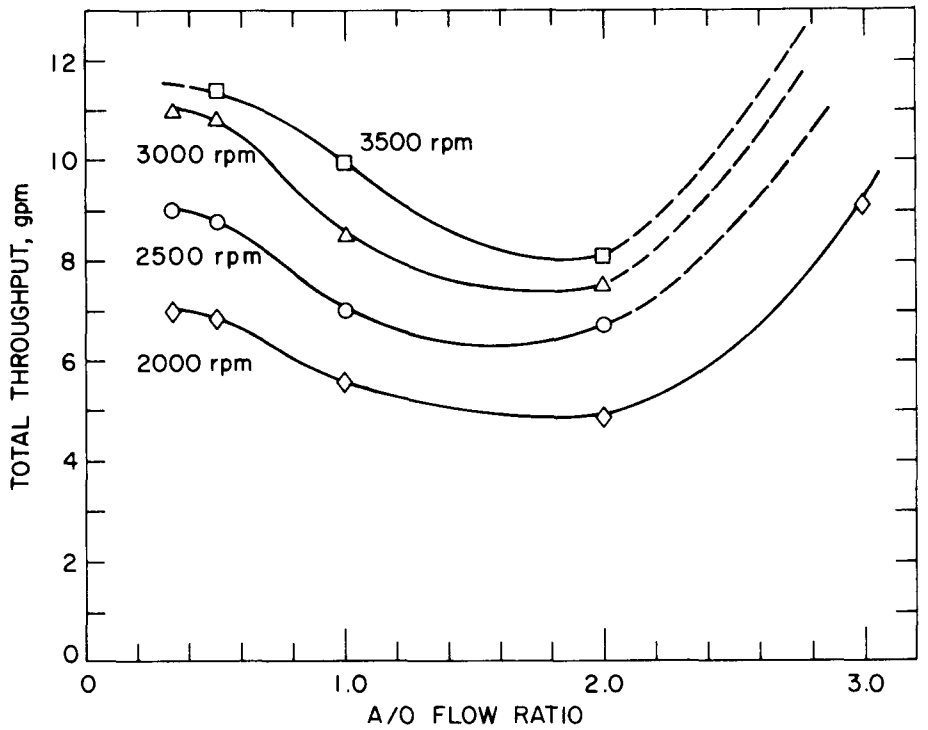

FIG. 14. Separating Capacity of Centrifugal Contactor with 4-in.-dia Rotor. Organic phase: 15% TBP in Ultrasene. Aqueous phase: 0.5M HNO_3. <1% entrainment.

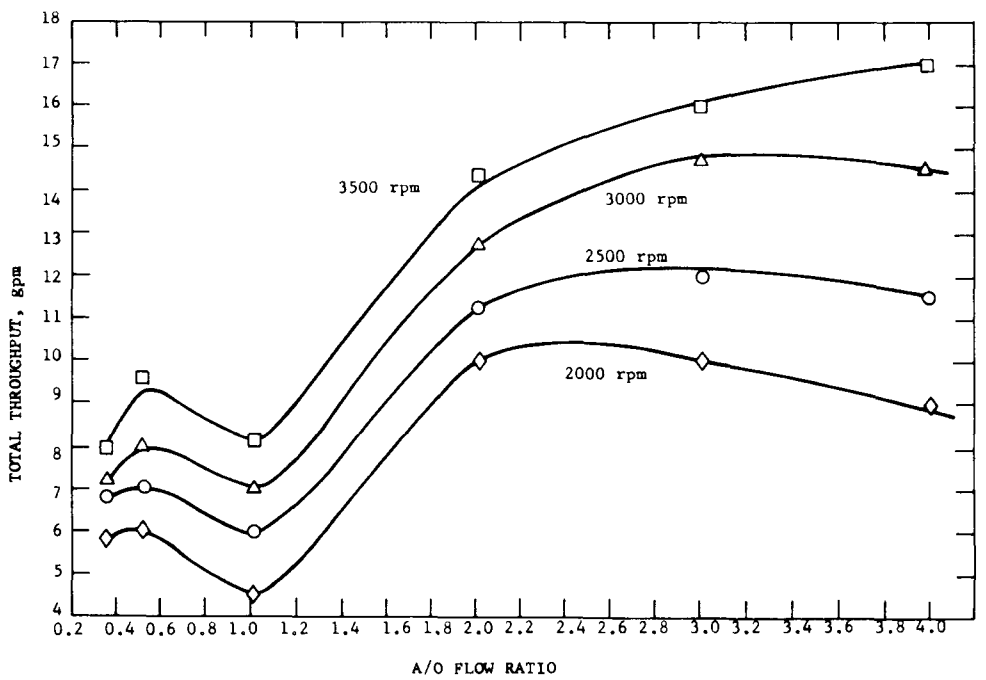

FIG. 15. Separating Capacity of Centrifugal Contactor with 4-in.-dia Rotor. Organic phase: 30% TBP in Ultrasene. Aqueous phase: 0.5M HNO_3. <1% entrainment.

In the course of these tests, a phenomenon identified as "surging" was noted. Surging manifested itself as a cyclic rise and fall in the flow rates of the effluent streams; in extreme situations, the amplitude of the cycles reached the point where effluent flows were essentially cut off momentarily. Surging is undesirable in a single contactor since it leads to (1) variation in the residence time of the mixed phases in the settling zone of the rotor and (2) oscillation of the position of the emulsion band. Both of these conditions can lead to increased contamination of the effluent streams and would require a reduction in flow rates. Surging in a bank of contactors operating in a countercurrent extraction system could cause excessive momentary variations in A/O ratios and thus lead to poor extraction efficiency.

A number of operating variances and equipment changes were examined in subsequent tests to establish the cause of surging and to lessen it. It was thought that when excessive pumping capacity existed, the mixing chamber tended to pump itself "dry" and lose its prime. The mixing chamber then effectively stopped pumping until it was essentially refilled with liquid, at which point it pumped again, at an excessive rate.

The changes made included increasing the number of baffles in the mixing chamber from 4 to 8 and removing the stabilizing ring from the paddle, adding a measured volume of air directly to the inlet tee, and permitting a controlled volume of air to flow through the casing drain line into the inlet tee. All of these techniques had the same general objective--to determine whether surging was due to the pumping capacity of the mixing chamber being substantially higher than the flow rate of solutions into the mixing chamber. It was observed that all of these changes tended to reduce the pumping capacity of the mixing chamber and ameliorate the problem of surging. Flow surging was eventually eliminated by using deeper paddles of smaller diameters and admitting air to the inlet tee through the casing drain line.

It is worthwhile noting that the problem of surging might be a result of the manner in which the contactor was tested. In the test facility, the inlet streams were essentially free of air; in an operating bank of contactors, the inlet streams would contain air entrained during spraying of streams out of the rotors of adjacent contactors. Consequently, in a bank of contactors, the mixing chambers would always operate in a "semi-primed" condition, and there would be less tendency for flow surging.

In other separating capacity tests, 0.5M HNO_3 was the aqueous phase and either 15 or 30% TBP in n-dodecane (NDD) was the organic phase. N-dodecane is currently the preferred diluent for Purex process flowsheets. Separating capacity was measured at rotor speeds of 2000 to 3500 rpm at aqueous to organic (A/O) flow ratios of 0.3 to 3.0 with 15% TBP, and at A/O flow ratios of 0.1 to 10 with 30% TBP. At all rotor speeds in the experiments with 15% TBP (Fig. 16), separating capacities were near their minimum values at A/O ratios of $\sim$2, as with the Ultrasene diluent. Capacities at an A/O ratio of 2 ranged from 5.5 gpm at 2000 rpm to 9.5 gpm at 3500 rpm. At an A/O ratio of 3, capacities ranged from 8 gpm at 2000 rpm to 15 gpm at 3500 rpm.

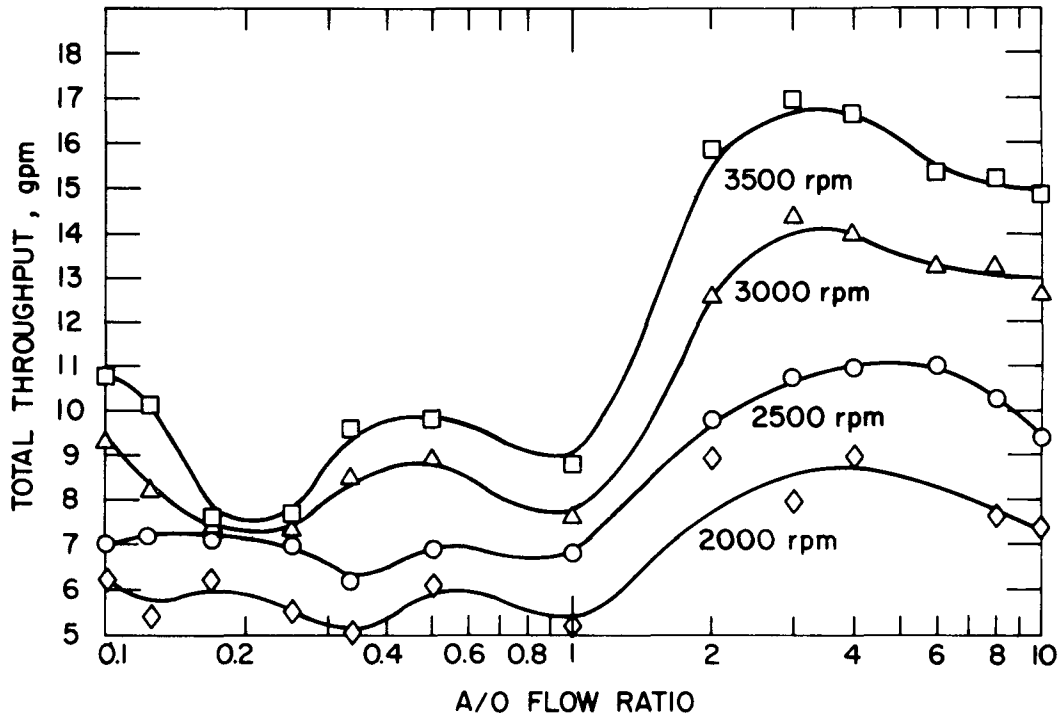

FIG. 16. Separating Capacity of Centrifugal Contactor with 4-in.-dia Rotor. Organic Phase: 15% TBP in n-dodecane. Aqueous Phase: 0.5M HNO_3. 1% entrainment.

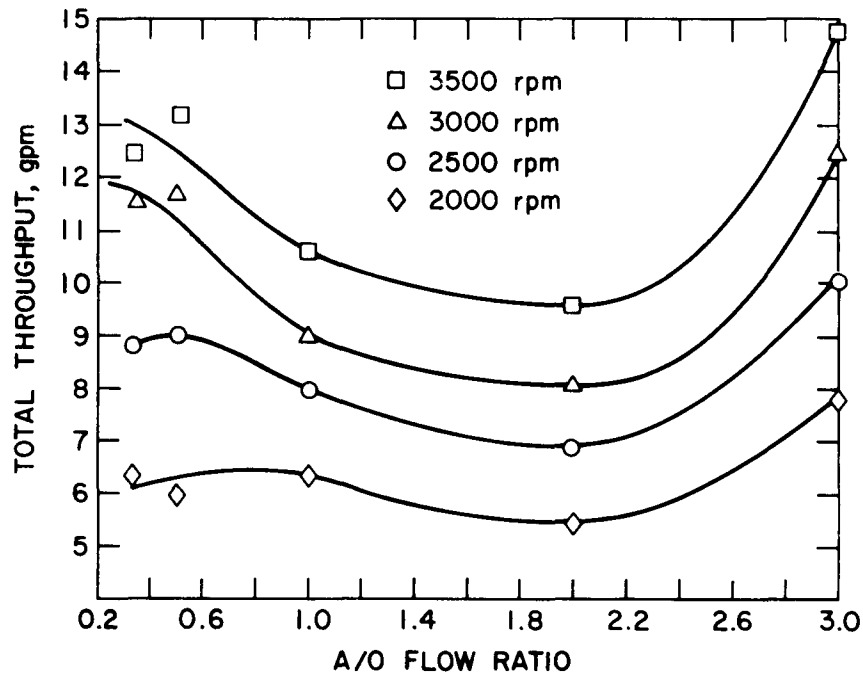

FIG. 17. Separating Capacity of Centrifugal Contactor with 4-in.-dia Rotor. Organic phase: 30% TBP in n-dodecane. Aqueous Phase: 0.5M HNO_3. 1% entrainment.

Test results for 30% TBP in n-dodecane are plotted in Fig. 17 on a semilogarithmic scale to accommodate the A/O flow ratios, which had a broader range than in the earlier tests. Minimum separating capacities were found at an A/O ratio of ∿1 and varied from 5 gpm at 2000 rpm to 9 gpm at 3500 rpm. Highest separating capacities were found at A/O ratios of 3 or 4 and ranged from 9 gpm at 2000 rpm to 17 gpm at 3500 rpm. As was true in the tests with Ultrasene diluent, capacities at A/O ratios below 0.4 or 0.3 were lower than at A/O ratios above 2 and did not follow quite as consistent patterns of variation with rotor speed. This is attributed mainly to differences in the kinds of emulsions formed. Overall separating performance in these tests was very similar to that found when Ultrasene was used as the diluent. A separating capacity of 5 gpm would be equivalent to a processing rate of somewhat more than 1 tonne/day of plutonium (or uranium) in a typical Purex process.

In these tests, an improved technique was employed to measure contamination of the effluent streams. Iniitally, entrainment was determined by collecting a 200-ml sample in a graduate and allowing it to stand for about 10 min. The quantity of contaminating phase was then read on the graduate scale. Since the amount of contamination of interest was less than 2 ml, the error in measurement could be significant as a result of either reading error or incomplete separation of very fine entrained material. In the improved sampling technique, a modified centrifuge tube was used. As shown in Fig. 18, a short length of burette tubing was added to the top of a tapered centrifuge tube. This change permitted the same tube design to be used to measure aqueous-phase contamination in the sample of organic phase effluent and organic-phase contamination in the sample of aqueous phase effluent.

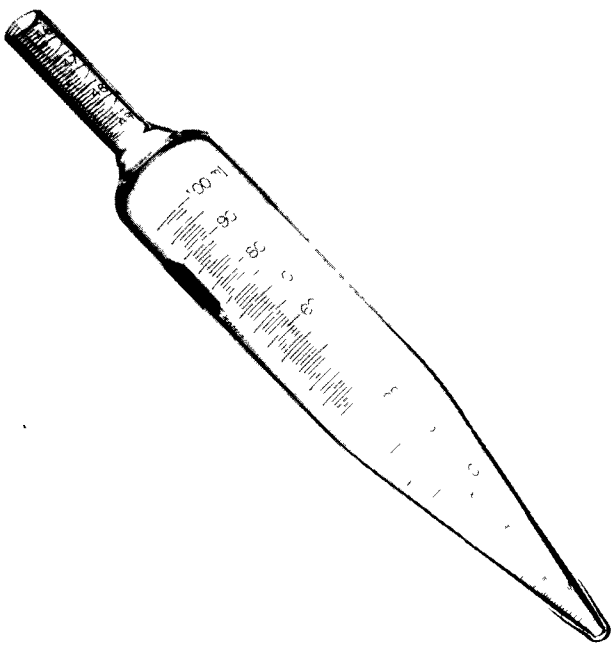

FIG. 18

Dual-Purpose Centrifuge Tube
(ANL Neg. No. 308-2844)

In measuring contamination with the improved technique, a pair of tubes holding about 115-ml samples was centrifuged for 15 sec at 1400 rpm in an International Centrifuge, Size 2.* Phase separation was complete, permitting accurate and rapid determination of contamination.

Surging continued to be investigated in the separating capacity tests with n-dodecane diluent. A new mixing paddle assembly was used that facilitated changes in paddle configuration. Various mixing paddle configurations were tested, as shown in Fig. 19. In the upper left of Fig. 19 is the original paddle after removal of the stabilizing ring. Also shown are the replaceable-blade paddle and two of the blade sections.

In addition, a spacer ring was inserted in the mixing chamber in some runs to determine any effect of mixing chamber volume on hydraulic stability and separating capacity. The ring was in the form of a cylindrical block with a central bore and occupied the lower section of the mixing chamber. Separating capacities remained essentially the same for the various mixing-chamber-volume/mixing-paddle combinations. However, hydraulic stability was improved when smaller diameter paddles were used in the larger volume mixing chamber. This result confirmed the earlier conclusion that a decrease in pumping capacity of the mixing chamber leads to more stable hydraulic operation.

During the above separating capacity tests, it was noted that at some feed rates, the rotor reached its maximum pumping capacity before it reached its maximum separating capacity. This condition was observed at high and low A/O ratios and not at intermediate A/O ratios. The result was a flooding condition: the casing annulus filled with emulsion that rose until it overflowed into the organic-phase collecting ring and contaminated the effluent organic stream. The pumping characteristics of the rotor were investigated to evaluate the nature of the problem. Also, the relationship between pumping capacity and separating capacity was investigated to determine if there is a basis for a practical limit of the L/D ratio in the rotor. Liquids are pumped up through the rotor as a result of the difference in pressure (developed by the centrifugal action of the rotor) between the inlet orifice at the bottom and the organic phase weir at the top. For a given rotor diameter, the separating capacity increases as the rotor length increases, but the pumping capacity decreases as the length increases. Thus, a limiting length is reached at which separating and pumping capacities are essentially equal; in rotors of greater length, pumping capacity would be reduced. For a rotor of the ANL design, the maximum effective L/D ratio appears to be about 4. (This subject is treated in more detail in Appendix D.)

B. Effect of Solids on Contactor Operation

Because of the small volume of the rotor, it is possible that a large enough quantity of solids from the feed stream will accumulate in the rotor of a centrifugal contactor so that the unit will become inoperable. Solids likely to appear in feed streams of a solvent extraction process are of

---

*Manufactured by International Centrifuge Equipment Co., Boston, Mass.

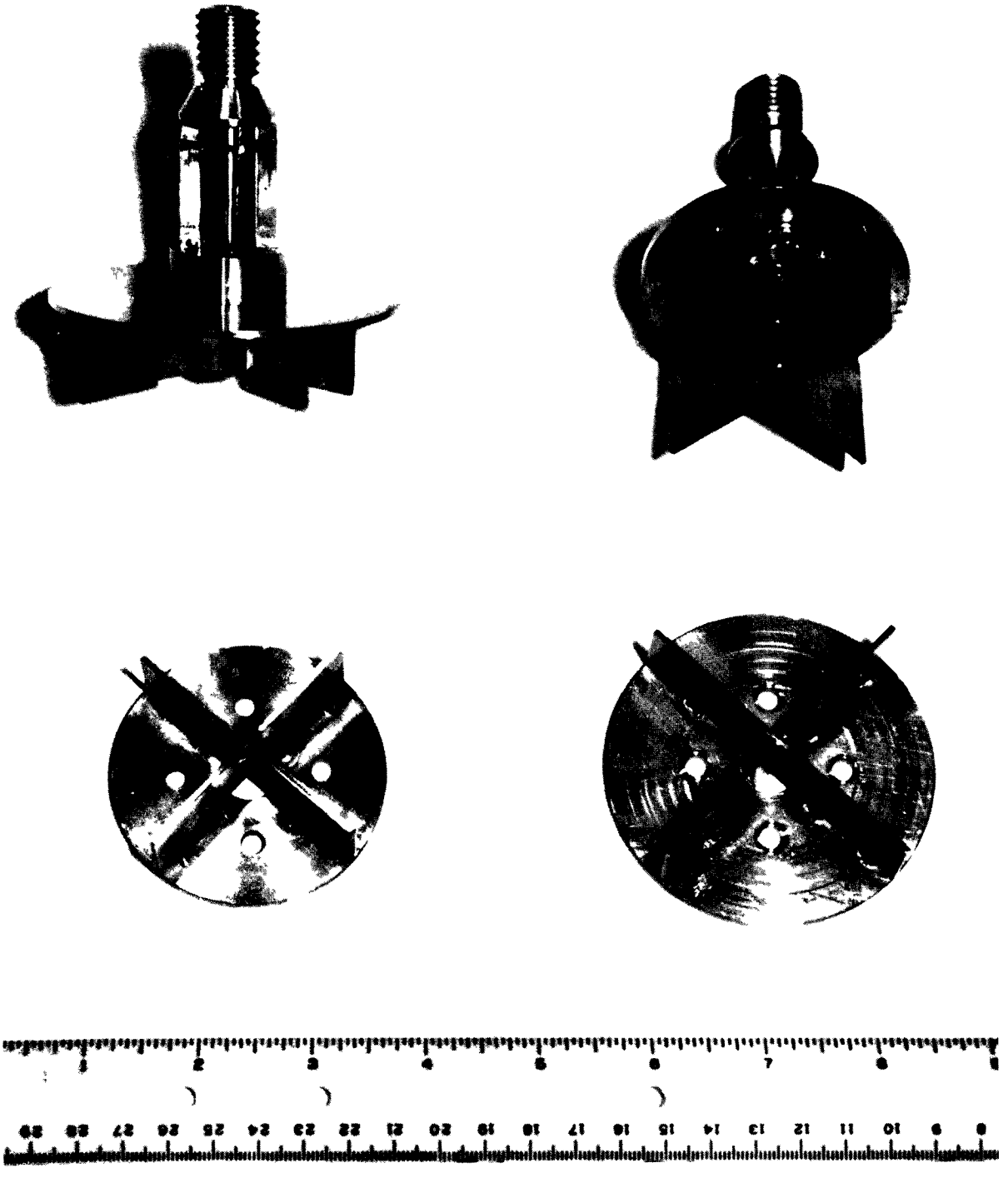

FIG. 19. Mixing Paddles Tested in Centrifugal Contactor Runs
(ANL Neg. No. 308-2849)

two kinds--fine, heavy particulate carried over from the dissolver and insoluble reaction products generally called "interface crud." It is the usual practice, in plants where fuel is processed by solvent extraction, to clarify the solution from the dissolver by centrifuging. This removes larger undissolved particulate solids.

At Savannah River,[6] the effect of solids in the feed was evaluated in tests with feed solutions containing various quantities of manganese dioxide. Freshly made MnO_2 tends to be quite flocculent and settles very slowly in an aqueous medium. Because the amount of MnO_2 that will collect in a rotor is sensitive to its physical form, widely varying amounts can accumulate in a centrifugal contactor. In a SR test in a multistage bank of 10-in.-dia contactors, the feed contained 5000 ppm of MnO_2. Approximately 2 kg accumulated in each unit when steady-state conditions had been reached (in comparison, only 25 g of MnO_2 had collected in similar single-stage tests). The presence of this large bulk of solids in the rotors did not affect the hydraulic performance of the contactors.

Two runs were made in the experimental ANL contactor with MnO_2 in the aqueous feed. The MnO_2 was prepared by adding NH_4OH to a solution of $KMnO_4$. Two concentrations of MnO_2 were used, and both tests were made at an A/O ratio of 1. The aqueous feed was 0.5M HNO_3 + MnO_2 and the organic feed was 30% TBP in n-dodecane. One run was made at 2000-rpm rotor speed and 4-gpm total throughput, the other run at 3500 rpm and 7-gpm throughput. (During these tests, the filter was absent from the aqueous supply pump line to avoid separation of MnO_2 from the circulated aqueous phase.)

In both runs, it was observed that MnO_2 appeared in the aqueous effluent stream immediately after startup, indicating that at no time was all suspended material separated from the aqueous phase. The relative concentration of MnO_2 in the aqueous effluent stream was determined periodically by centrifuging 115-ml samples and observing the level of settled solids. After about 30 min of operation, the quantity of MnO_2 in the effluent stream levelled off and appeared to be equal to the quantity in a feed solution sample. After about 1 hr of operation, 1-liter samples of the feed solution and the aqueous phase effluent stream were taken and filtered. The solids were dried and weighed to establish that an equilibrium condition had been achieved. No MnO_2 solids were observed in the organic phase effluent stream in any of the tests. Following each test, the MnO_2 that had accumulated in the rotor was removed by flushing with water and then with oxalic acid and nitric acid.

Results are tabulated in Table 1. These results show that even with the very high solids loading in the feed, relatively little material was retained in the rotor. No operating difficulties were encountered in these runs, and it is quite reasonable to assume that no difficulties would be caused by the much lower concentration of interface crud likely to be found during Purex-type processing.

Table 1. Summary of Contactor Runs with MnO_2 Solids (SR Mixing Mode)

	Run 124A	Run 124B
MnO_2 conc. in feed, ppm	2600	2400
Total feed rate (A/O = 1), gpm	4	7
Rotor speed, rpm	2000	3500
Running time, min	70	85
Aqueous throughput, gal	140	300
Retained MnO_2, g	83	105

C. Determination of Extraction Efficiency

Extraction efficiency of the centrifugal contactor was determined by measuring the amount of uranium transferred from a nitric acid aqueous phase to an organic phase of 30% TBP in n-dodecane. Since only a single-stage contactor was being tested, no attempt was made to duplicate Purex process operation conditions. The composition of the aqueous stream (0.463M U, 0.68M HNO_3) was selected to give concentrations convenient for analysis.

A set of five tests was conducted, with each test following immediately after the preceding test. Stock solutions were prepared in the supply tanks of the test facility (see Fig. 8). Approximately 20 gal of each phase was then pumped into its overhead tank, which served as a supply tank. During a test, the inlet streams flowed by gravity through the rotameters to the contactor and out into the collecting tanks. Flowrates were regulated by valves on the inlet lines. The extraction runs were all made at A/O = 1. The smallest-diameter paddle (2 1/2-in.-dia by 1 3/8-in.-high blades) was used, since this paddle produced the least vigorous mixing.

Flowrates, weir pressure, and rotor speed were adjusted as specified for a given run. Since the contactor achieves steady-state operation in well under one minute, it was possible to make a set of five runs in about five minutes. At each run condition, samples of effluent streams were taken before conditions were changed to those for the next run. Equal-volume aliquots of effluent samples from each run were equilibrated by vigorous shaking to obtain data on uranium concentration in both phases at equilibrium.

Stage efficiencies, E_A, were determined on the basis of aqueous compositions using the equation:

$$E_A = \frac{A_i - A_o}{A_i - A_e} \times 100 \qquad (4)$$

where A_i = U concentration, M, in aqueous feed
A_o = U concentration, M, in aqueous effluent
A_e = U concentration, M, in aqueous effluent after equilibration with an equal volume of organic effluent

All samples were analyzed using colorimetric analyses (for which results are accurate within about 2-3%).

Extraction efficiencies based on organic sample composition, E_o, were determined using the equivalent formula

$$E_o = \frac{O_o - O_i}{O_e - O_i} \times 100$$

where O_o = U concentration, M, in organic effluent
O_i = U concentration, M, in organic feed
O_e = U concentration, M, in organic effluent after equilibration with an equal volume of aqueous effluent

Values of E_o and E_A and average E values are summarized in Table 2.

Table 2. Stage Efficiencies for Uranium Extraction. Run UXS-1

Aqueous Phase: 0.463M U, 0.68M HNO_3
Organic Phase: 30% TBP in n-dodecane
A/O: 1

Run UXS-	Rotor Speed, rpm	Total Feed Rates, gpm	% of Maximum Separating Capacity[a]	E_A, %	E_o, %	E_{ave}, %
1a	2000	4	75	100	98	99
1b	2500	4	60	103	97.6	100.3
1c	3000	4	50	103	96.1	99.5
1d	3000	7	90	97.7	100.5	99.1
1e	3500	7	80	99.0	96.0	97.5

[a]Maximum separating capacity determined in tests without uranium.

Examination of the data in the table shows that stage efficiency in every run was essentially 100%. It is clear that excellent phase mixing was achieved, even under conditions of relatively low mixer speed. Since residence times in the mixing chamber were less than 2 sec, these tests demonstrate the very rapid attainment of equilibrium in uranium extraction. Material balances based upon the assumption of equal solution flow rates ranged between 96 and 102%, indicating that the A/O ratio of 1 was very closely maintained during the run.

VI. DISCUSSION AND CONCLUSIONS

The mechanical performance of the unit was excellent, demonstrating that the problem of operating at high speeds in a long-rotor contactor can be solved by careful attention to design and fabrication tolerances. The problems related to flow surging were corrected by decreasing the pumping capacity of the mixing chamber while retaining adequate mixing intensity for high extraction efficiency.

A correlation (Eq. 1) relating separating capacity to rotor speed, rotor ID, the settling length of the rotor, the mixing paddle speed, and the mixing paddle diameter has been shown to hold for a wide range of sizes of centrifugal contactors of the Savannah River type. However, the tests with various paddle sizes showed that separating capacity was not significantly affected when paddle diameters varied from 2 1/2 in. to 3 1/4 in. The effect of paddle diameter may have been offset partly by the fact that the smaller-diameter paddles had wider blades. Thus, although Eq. 1 indicates that separating capacity is inversely proportional to mixing paddle diameter, this effect can be largely eliminated by adjusting paddle blade width along with paddle diameter. Since the mixing intensity is high, it is possible that changes in paddle diameter do not significantly affect the type of emulsion formed. If the mixing chamber were designed with small clearances between the paddle and the baffles, the very high shear produced with larger-diameter paddles might result in a decrease in separating capacity.

Although no definitive study of nuclear criticality considerations was performed, a basis was established for the design of a multistage assembly. It was shown that the diameter of the collecting zone of a centrifugal contactor could be reduced to a critically safe dimension and still be capable of handling the required volume of effluent. The allowable overall dimensions for a given unit can best be evaluated in relation to the specific solutions to be processed and the number of stages required.

The length-to-diameter (L/D) ratio employed in the rotor is about twice as great as was used heretofore in contactors of the Savannah River type. The contactor retains the desirable features of the SR units--low holdup, quick attainment of a steady-state conditions, rapid flushout at the end of a processing campaign, and reduced radiation damage to the solvent. Hydraulic performance was excellent. It has been demonstrated that a high-capacity, critically safe contactor of relatively large L/D can be built and operated. The high stage efficiency observed in uranium extraction indicates that units of this type would be highly suitable for solvent extraction processing of high-plutonium-content fast reactor fuels.

Early work at Savannah River[13] indicated that the high plutonium losses and poor decontamination generally associated with Purex processes in which the solvents are highly irradiated could be largely avoided in short-residence-time contactors. This finding suggests that kinetic factors may be very significant in affecting the quality of separations. Thus, separation processes may be developed based upon significant differences in extraction kinetics, as observed by Russian workers,[12]

as well as differences in distribution coefficients. A possible application of this idea in a Purex-type process would be to use contactors with small mixing chambers in the extraction section and extractors with larger mixing chambers in the scrub section. This combination might reduce the quantity of fission product extracted with the plutonium and yet improve fission product removal in the scrub section. This represents an area for future study.

APPENDIX A. NUCLEAR CRITICALITY

A primary objective in the ANL centrifugal contactor program was to develop a unit that has a high separating capacity and is geometrically safe against nuclear criticality when solutions with high concentrations of plutonium are processed. Since a centrifugal contactor is essentially cylindrical, the separating capacity is very significantly affected by the diameter of the rotor (see Appendix D). Accordingly, in designing the contactor, the largest safe rotor diameter was selected. To increase separating capacity further, the length and speed of the contactor rotor were increased.

The contactor under development was to be evaluated for application to plutonium isolation steps (the second and third cycles) of a Purex-type solvent extraction process for LMFBR fuel. It was expected that the contactor would have a capacity suitable for the plutonium cycles of a 5 tonne/day (U + Pu + FP) processing plant. In the first generation of LMFBRs, it is expected that a mixed oxide having a nominal composition of UO_2-20% PuO_2 will be the fuel in the core. Consequently, the amount of plutonium to be processed was expected to be about 1 tonne/day.

In evaluating the criticality aspects of the contactor design, certain conservative assumptions were made that reduced the maximum allowable diameter of the contactor:

1. The concentration of plutonium in the aqueous phase was no greater than 200 g/liter.
2. No ^{240}Pu, ^{238}U, or HNO_3 was present. (Some HNO_3 would always be present and some ^{240}Pu would almost certainly be present in any irradiated fuel.)
3. No fixed or soluble nuclear poisons were present.
4. Full water reflection.

The general shape of the ANL experimental contactor is as shown in Fig. 1. Another assumption that tended to reduce the maximum allowable diameter was related to hypothetical operating conditions of the contactor, namely, that the entire contactor, including the collecting rings, might be filled with concentrated aqueous solution (containing 200 g Pu/liter). However, this condition could not occur during normal operation of the contactor since (1) there is a hollow core in the center of the rotor, (2) the collecting rings are only partially full, and (3) the contactor contains some organic phase (30% tributyl phosphate in n-dodecane or another diluent) whose plutonium concentration cannot reach 200 g/liter. When the contactor (or a bank of contactors) is idle, it is extremely unlikely to be filled with aqueous feed solution (as from a leaky feed supply system) for the following reasons: There are no shut-off valves in the effluent lines, and liquid in the upper section of an idle contactor would drain by gravity to the level of the organic phase outlet. In addition, the internal rotor assembly reduces the available open volume of the contactor.

Based on the above conservative assumptions, the lower section of the contactor casing was treated as an infinite cylinder for criticality consideration. The maximum geometrically safe diameter of an infinite cylinder [assuming plutonium present as $^{239}Pu(NO_3)_3$] is given by Clark[10] as 5.37 in. It is reasonable to assume that the maximum critically safe diameter of a container for $Pu(NO_3)_4$ would not be less. To provide an additional margin of safety, the ID of the cylindrical casing of the contactor was reduced to 4.75 in. (In a subsequent change in which the contactor was modified to permit operation in a different mixing mode, the ID of the bottom portion of the casing was enlarged to 5.2 in. The contactor of modified design is the subject of a companion topical report.[8])

As shown in Fig. 1, the upper section of the casing has a larger diameter than does the lower section to provide space for the aqueous and organic phase collector rings. Since initial efforts in the development of the long-bowl, small-diameter contactor were directed at investigating its separating capacity and hydraulic characteristics, it was not considered necessary to limit the diameter of the collector section to a geometrically safe dimension; consequently, its ID was 7 in.

Experience gained in testing the contactor showed that as much as 13 gpm could be handled by the aqueous phase collector without spillover into the organic phase collector. Since a contactor designed for handling 1 tonne/day of plutonium would probably operate at less than 5 gpm total throughput, it is unlikely that the flow rate of either phase would be more than 3 or 4 gpm. Such a flow could easily be handled by collector rings no greater than 5.37 in. in diameter, particularly if the inside diameter of the collector ring were made somewhat smaller than in the present design and the tangential discharge lines were made somewhat larger.

Accordingly, it is reasonable to conclude that a centrifugal contactor with a 4-in.-ID rotor can be built in a critically safe configuration. This evaluation does not take into consideration the effect of interactions between adjacent contactors in a bank of six or eight units, nor does it allow for the effect of interconnecting pipes. These more rigorous determinations were properly postponed until a specific contactor size is selected for a specific process and performance. If necessary, a modest reduction in casing and rotor diameters could be made to allow for multi-unit interactions. The effects of dimensional changes on contactor capacity could be estimated on the basis of the separating capacity correlation discussed in the body of this report.

APPENDIX B. CRITICAL SPEED CALCULATIONS FOR ROTOR ASSEMBLY

The rotor diameter of the ANL centrifugal contactor was limited by criticality considerations (see Section II and Appendix A of this report). The total length of the rotor (weir section plus separating section) was limited by critical speed considerations to ensure safe operation at test speeds up to 3500 rpm. Calculations were made to determine the approximate first critical speed of the rotor assembly as a function of its total bowl length. In making these calculations, the following equation[11] was used:

$$N_{cs} = 167.6/(\Sigma\Delta)^{1/2} \tag{5}$$

where N_{cs} = first critical speed, rpm
$\Sigma\Delta$ = sum of static deflections, in.

The sum of the static deflections was calculated by considering the rotor assembly to be a nonuniform beam rigidly supported at one end as illustrated in Fig. 20. (The rotor is shown in the horizontal position rather than its normal vertical operating position.) As shown in Fig. 20, the 1 1/4-in.-dia rotor shaft was assumed to extend 1 in. above and 2 in. below the tubular bowl section which has a length, L_B. The 2-in. length of shaft extended below the bowl was considered to have at least as great an effect during operation on the calculated static deflection as does the mixing paddle shaft and paddle (Fig. 1).

The area moment method[14] was used to calculate the static deflections at the free end of the shaft due to (1) the 1-in. length of 1 1/4-in.-dia shaft above the bowl (Δ_1) and (2) the slotted weir section at the top of the bowl (Δ_2). The deflection at the unsupported end of the shaft due to the tubular bowl section (Δ_3) was calculated from the general deflection formula for a uniformly loaded cantilever beam. Substitution of ($\Delta_1 + \Delta_2 + \Delta_3$) for ($\Sigma\Delta$) in Eq. 5 gives

$$N_{cs} = 167.6/(\Delta_1 + \Delta_2 + \Delta_3)^{1/2} \tag{6}$$

Calculations were made for each of the three static deflections as a function of the total bowl length, L_B. The relative contribution of each of the three deflections to the total static deflection is shown in Fig. 21.

1. Calculation of Δ_1

In order to estimate the load, P, at the end of the 1-in. length of shaft above the bowl, the total bending moment on the supported end of the shaft was calculated, assuming the rotor assembly to weigh 30 lb and to be 20 in. long. Based on these assumptions, the total bending moment was calculated from the following equation:[11]

$$M = W_R \ell/2 \tag{7}$$

where M = bending moment, in.-lb
W_R = weight = 30 lb.
ℓ = length of rotor assembly = 20 in.

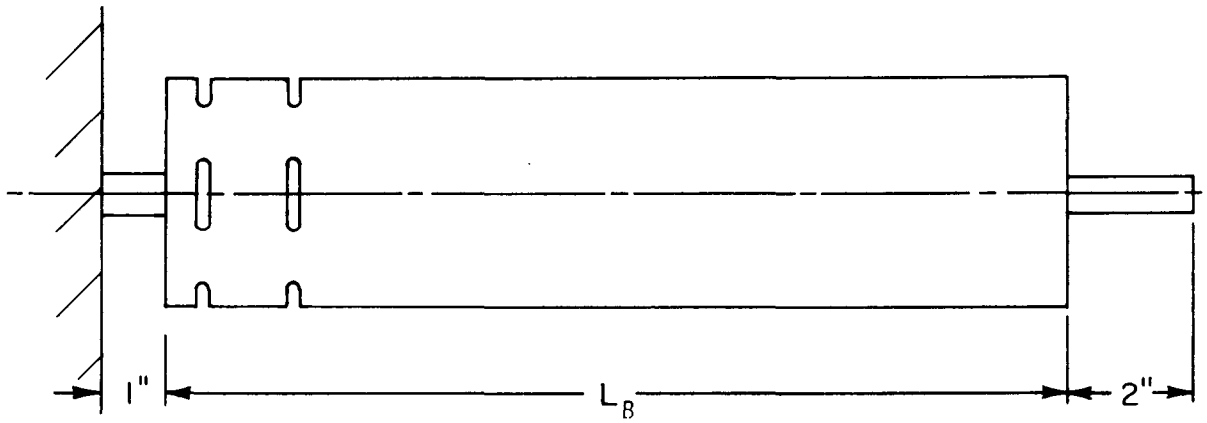

FIG. 20. Schematic Drawing of Rotor and Shaft Assembly

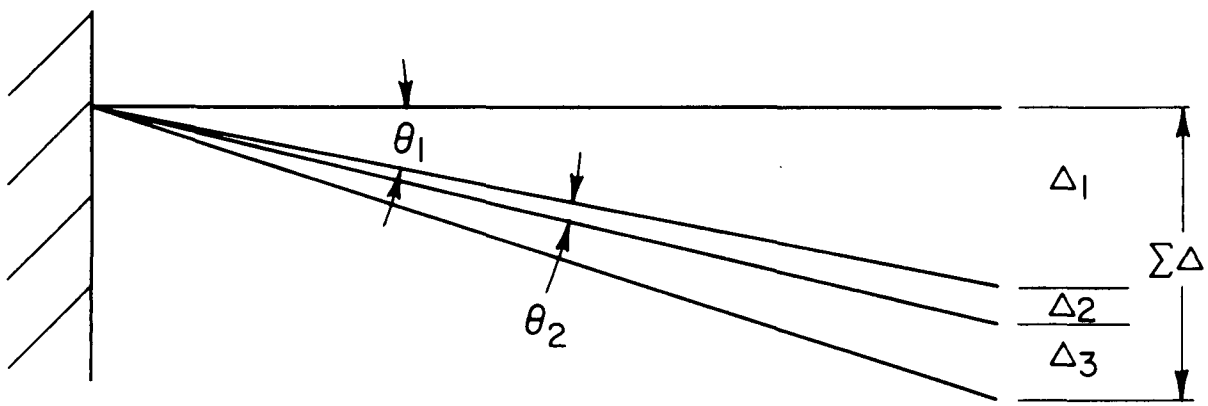

FIG. 21. Static Deflection of Rotor as a Function of Bowl Length

Solving for M, the total bending moment equals 300 in.-lb and the load required to produce an equivalent bending moment at the end of the 1-in. length of the shaft is about 300 lb.

The slope, θ, of the deflected shaft at the free end of the 1-in. length of shaft was calculated using the following equation:[15]

$$\tan \theta_1 = dy_1/dx_1 = P\ell_1^2/2\ EI \tag{8}$$

where P = load = 300 lb
ℓ_1 = length = 1 in.
E = modulus of elasticity = 29×10^6 psi (for stainless steel)
I = moment of inertia = 0.12 in.^{4} (for 1 1/4-in.-dia shaft)

Solution of Eq. 8 yields

$$\tan \theta_1 = 43.2 \times 10^{-6}$$

The deflection at the unsupported end of the rotor assembly due to the 1-in. length of shaft above the bowl can be expressed as a function of the total bowl length, L_B, as follows:

$$\Delta_1 = \tan \theta_1\ (L_B + 2)\ \text{in.} \tag{9}$$

Therefore,

$$\underline{\underline{\Delta_1 = 43.2 \times 10^{-6}\ (L_B + 2)\ \text{in.}}} \tag{10}$$

2. Calculation of Δ_2

The same assumptions as were used to determine Δ_1 were used to calculate the deflection, Δ_2, at the unsupported end of the rotor assembly due to the slots in the weir section of the bowl. Equation 8 was rewritten to determine the slope of the deflected shaft at the slots as follows:

$$\tan \theta_2 = dy_2/dx_2 = P\ell_2^2/2\ EI \tag{11}$$

where P = load = 300 lb (assume same value as for calculation of Δ_1)
ℓ_2 = length of slots = 0.75 in.
E = 29×10^6 psi (as in equation 8)
I = 1.33 in.^{4} (due to symmetry, calculated about the axis through only two of the four slots)

Solution of Eq. 11 yields

$$\tan \theta_2 = 2.18 \times 10^{-6} \tag{12}$$

The deflection at the unsupported end of the rotor assembly due to the 0.75-in. length of the slots in the weir section can be expressed as a function of the total bowl length, L_B, as follows:

$$\Delta_2 = \tan \theta_2\ (L_B + 1.25)\ \text{in.} \tag{13}$$

Therefore,

$$\underline{\underline{\Delta_2 = 2.18 \times 10^{-6} \ (L_B + 1.25) \text{ in.}}}$$

3. Calculation of Δ_3

The deflection, Δ_3, at the unsupported end of the rotor assembly due to the tubular bowl section was calculated as a function of the total bowl length, L_B. For this calculation, the following equation[11] for the deflection of a uniformly loaded cantilever beam was used:

$$\Delta_3 = W\ell_3^3/8 \ EI \tag{14}$$

where W = weight = $2.81 + 1.26 \ L_B$, lb
ℓ_3 = length = $(L_B + 2)$, in.
$E = 29 \times 10^6$ psi (as in equation 8)
$I = 2.34$ in.^{4} (for tubular section)

Substitution of the above values in Eq. 14 gives

$$\Delta_3 = (2.81 + 1.26 \ L_B) \ (L_B + 2)^3/(8) \ (29) \ (10^6) \ (2.34) \text{ in.} \tag{15}$$

Simplifying yields

$$\underline{\underline{\Delta_3 = (2.81 + 1.26 \ L_B) \ (L_B + 2)^3/5.44 \times 10^8 \text{ in.}}}$$

4. First Critical Speed of Rotor Assembly

The expressions derived for Δ_1, Δ_2, and Δ_3 were substituted in Eq. 6, and a computer program was set up to calculate the first critical speed (N_{cs}) of the rotor assembly for various bowl lengths, L_B, between 11 in. and 16 in. Based on the results of these calculations, a bowl length of 15 in. (3-in. weir section and a 12-in. separating section) was selected for the ANL contactor. The calculated first critical speed for this 15-in. bowl length was about 5400 rpm. Several conservative assumptions were made in calculating this critical speed. As a result, the actual critical speed of the unit is believed to be greater than the calculated 5400 rpm. For example, no benefits were assumed for the stiffening effects due to the 1 1/4-in.-dia center shaft through the bowl, the welded-disk construction of the 3-in.-high weir section, and the four skip-welded radial vanes in the separating section. For safe operation of high-speed equipment, it is recommended that operating speed not exceed approximately 70% of the calculated first critical speed. In repetitive testing of the contactor at speeds up to 3500 rpm, as well as in a few short-duration tests at speeds up to 4000 rpm, no mechanical instabilities were detected that would indicate the unit was approaching its first critical speed.

APPENDIX C. CALCULATION OF AIR-WEIR PRESSURES

The ANL centrifugal contactor was designed with an air-controlled aqueous-phase weir to vary the position of the emulsion band (or interface) that is formed in the separating section between the heavy aqueous phase and the light organic phase. Mathematical expressions were derived[3,6] for calculating the air weir pressure as a function of rotor speed, aqueous and organic flow rates, and aqueous and organic phase densities. The various radii used in the mathematical expressions are identified in Fig. 22 (reproduced from reference 6).

Due to criticality considerations, the inside diameter of the rotor in the ANL contactor was limited to 4 in. The radial distance of each weir and baffle from the center of the 1 1/4-in.-dia shaft of the ANL unit is as follows:

Weir or Baffle	Radial Distance, in.
Two aqueous baffles (r_{uf})	1.75
Two aqueous weirs (r_{a*})	1.375
Organic weir (r_{o*})	1.0

The flow of aqueous and organic phases through the weir section of the rotor can be understood by inspection of Fig. 3 of this report. The aqueous phase leaves the disengaging section through the 1/4-in. annular gap between the lower aqueous underflow baffle (r_{uf}) and the internal radius (2 in.) of the rotor. The organic phase (plus any entrained air entering the contactor) leaves the disengaging section through the 3/8-in. annular gap between the organic weir (r_{o*}) and the 5/8-in.-radius shaft. The aqueous weir (r_{a*}) is located halfway between the lower aqueous underflow baffle (r_{uf}) and the organic weir (r_{o*}) for flexibility in testing the contactor's performance at various rotor speeds, total flow rates, aqueous-to-organic flow ratios (A/O), and aqueous and organic phase densities.

In the derivation of the mathematical expressions for liquid flow over the edge of a circular weir in a centrifugal field, the aqueous weir was treated as a sharp-edge weir and the organic weir as a broad-crested weir. The generally accepted weir coefficients (k_*) are 0.415 for a sharp-edge weir and 0.33 for a broad-crested weir.[16] These values do not take into account the Coriolis effect encountered in a centrifugal field. The relationships between the actual circular weir coefficient in a centrifugal field (k) and the generally accepted weir coefficient (k_*) for the aqueous and the organic weirs are given in the following equations:

$$\ln (k_a/k_{a*}) = -(4/b_a n)(k_{a*} f\pi)^{2/3} (q_a/\omega_1)^{1/3} \tag{16}$$

and

$$\ln (k_o/k_{o*}) = -(4/b_o n)(k_{o*} f\pi)^{2/3} (q_o/\omega_1)^{1/3} \tag{17}$$

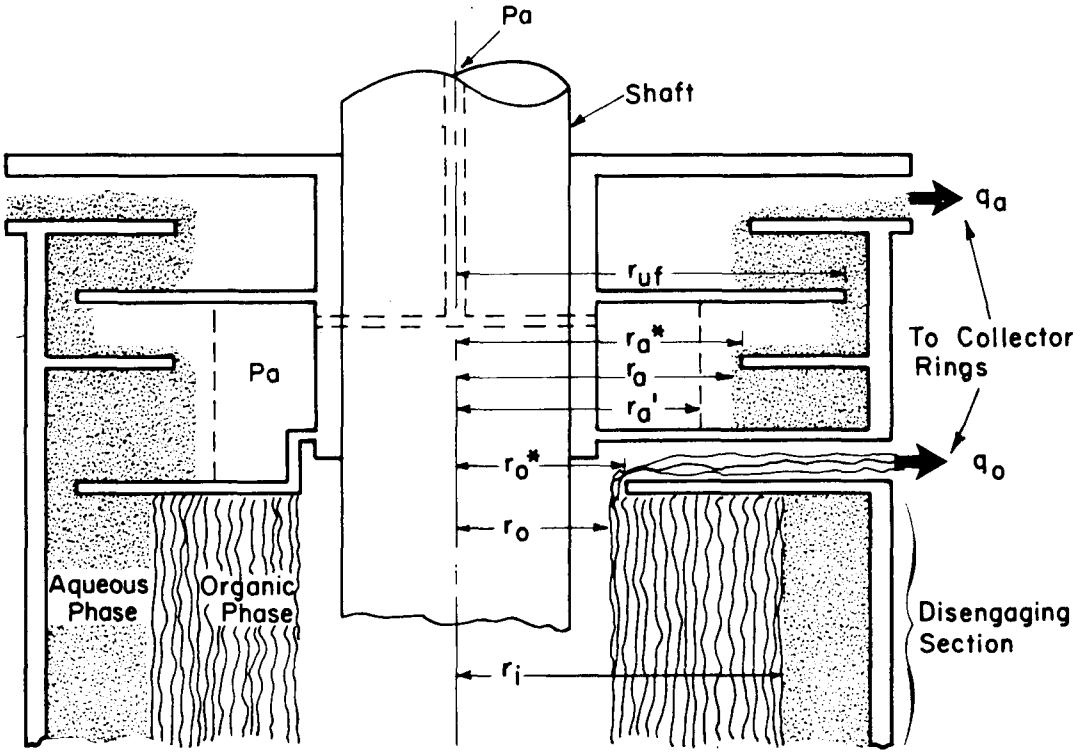

FIG. 22. Interface Control Weirs of Centrifugal Contactor
(Modified version of figure on p. 23, Ref. 6)

where, for the ANL contactor:

k_a = actual aqueous-phase circular weir coefficient in centrifugal field
k_o = actual organic-phase circular weir coefficient in centrifugal field
k_{a*} = 0.415 for a sharp-edge aqueous weir
k_{o*} = 0.33 for a broad-crested organic weir
b_a = 1 in. = height of disengaging section for aqueous phase
b_o = 12 in. = height of disengaging section for organic phase
n = 4 = number of radial vanes
f = 0.95 = assumed fraction of circumference available for flow
q_a = flow rate over aqueous weir, in.^{3}/min
q_o = flow rate over organic weir, in.^{3}/min
ω_1 = angular velocity, radians/min

Since the rotor speed, the aqueous flow rate, and the organic flow rate for a given system are generally known, the actual liquid radius at the aqueous and the organic weirs can be determined from the following equations:

$$r_a = [r_{a*}^2 - (q_a/k_a f \pi \omega_1)^{2/3}]^{1/2} \tag{18}$$

and

$$r_o = [r_{o*}^2 - (q_o/k_o f \pi \omega_1)^{2/3}]^{1/2} \tag{19}$$

where, for the ANL contactor:

r_a = actual liquid radius at aqueous weir, in.
r_o = actual liquid radius at organic weir, in.
r_{a*} = 1.375 in. = physical radius of aqueous weir
r_{o*} = 1.0 in. = physical radius of organic weir

Having determined the actual liquid radius at the aqueous and the organic weirs (r_a and r_o) for a given set of conditions, the added air weir pressure (P_a) required to properly position the aqueous-organic emulsion band between the lower aqueous underflow baffle (r_{uf}) and the organic weir (r_{o*}) can be calculated from the following expression:

$$P_a = \frac{\omega_1^2 \rho_a}{2 g_c (60)^2 (12)^4} [r_a^2 - \frac{\rho_o}{\rho_a} r_o^2 - (1 - \frac{\rho_o}{\rho_a}) r_i^2] \tag{20}$$

where: P_a = air weir pressure, psig
g_c = force conversion factor = 32.2 (lb mass/lb force)(ft/sec^2)
ρ_a = density of aqueous phase, lb/ft^3
ρ_o = density of organic phase, lb/ft^3
r_i = radius of interface between two clear phases in disengaging section with no emulsion present, in.

By the use of Eq. 20, values of the air weir pressure, P_a, were computed for rotor speeds of 2000 to 3500 rpm, for total flow rates of 2 to 20 gpm, for aqueous-to-organic flow ratios (A/O) of 0.1 to 10, for aqueous densities of 1 to 1.3 x 62.4 lb/ft^3, and for organic densities of 0.7 to 0.95 x 62.4 lb/ft^3. In the compution of P_a, a value of 1.42 in. was assumed for the interface radius, r_i. This value is the volumetric mean radius of a hypothetical interface between equal volumes of clear aqueous and organic phases. It is assumed to be representative of the condition that exists when the entrainment of each phase in the other phase leaving the disengaging section has reached the maximum allowable level of 1 vol %. Under this condition, the width of the emulsion band is at a maximum; i.e., the emulsion band extends from the organic weir (r_o*) outward to the lower aqueous underflow baffle (r_{uf}).

For the various systems tested under these conditions, the experimental air weir pressures required to properly position the emulsion band were found to be in good agreement with the calculated values. As an example of this agreement, values of the air weir pressure calculated from Eq. 20 together with the experimental air weir pressures required to achieve maximum separating capacity for one system tested are listed in Table 3.

Table 3. Calculated and Experimental Air-Weir Pressures

Aqueous Phase: 0.5M nitric acid (sp gr, 1.015)
Organic Phase: 15 vol % TBP in n-dodecane (sp gr, 0.786)
Aqueous-to-Organic Flow Ratio: 1.0

Rotor Speed, rpm	Maximum Separating Capacity, gpm	Weir Air Pressure (P_a), psig	
		Calculated	Experimental
2000	6.4	1.09	1.0
2500	8.0	1.71	1.7
3000	9.0	2.50	2.6
3500	10.6	3.40	3.5

A generalized plot of the required air weir pressure as a function of the total throughput for a centrifugal contactor with an air-controlled weir is illustrated in Fig. 23. For a given set of conditions, the maximum separating capacity is represented in the figure by point C, the convergence of curves A and B. Curve A indicates air weir pressure as a function of total throughput for 1% aqueous in the organic effluent and <1% organic in the aqueous effluent. Curve B indicates the air weir pressures as a function of total throughput for 1% organic in the aqueous effluent and <1% aqueous in the organic effluent.

In determining the maximum separating capacities of various systems in the ANL contactor, no attempt was made to locate the air weir pressures along curves A and B. Instead, the air weir pressure was adjusted as required as the total throughput was increased until the maximum separating capacity represented by point C of Fig. 23 was reached.

In normal operation, centrifugal contactors are run at about 70 to 80% of their maximum separating capacity to ensure uncontaminated effluent streams. This normal operating range is illustrated by the shaded area of Fig. 23. As the total throughput is reduced below the throughput for maximum separating capacity, the allowable range of air weir pressures for efficient separation of the two phases increases. Consequently, a common air supply can be used for a bank of contactors to achieve efficient separation of the phases, even though minor variations occur in the operating conditions of the individual contactors of the bank. The changes in phase densities that result from the variation in uranium concentration from stage to stage are essentially self-compensating. Since high uranium or plutonium concentrations occur simultaneously in both phases of a given contactor, the ratio of phase densities does not change drastically. For example, in the uranium extraction tests made with the ANL contactor, air weir pressures were 0.1 psi higher than the pressures used when no uranium was present.

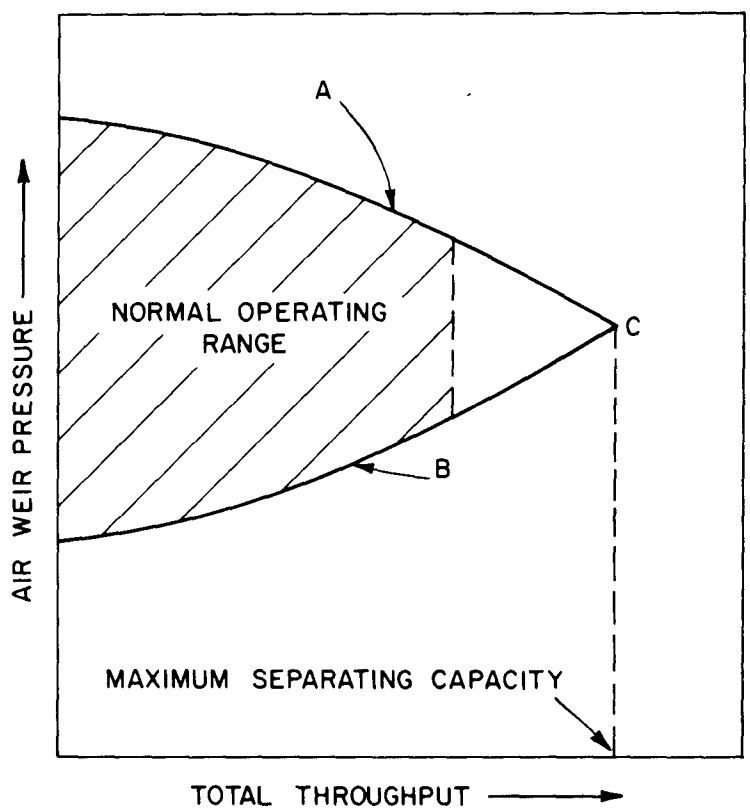

FIG. 23. Air-Weir Pressure as a Function of Total Throughput. Curve A, 1% Aqueous Phase in Organic Effluent and <1 vol % Organic in Aqueous Effluent. Curve B, 1% Organic Phase in Aqueous Effluent and <1 vol % Aqueous in Organic Effluent. Point C, 1% Aqueous in Organic Effluent and 1 vol % Organic in Aqueous Effluent.

APPENDIX D. ROTOR PUMPING CAPACITY

In Section II of this report, an expression for estimating the separating capacity of a centrifugal contactor was used which has the form:

$$\text{Separating Capacity, gpm} \propto \frac{N_c^2 D_b^3 L}{10^5 \, N_m D_m} \tag{21}$$

where N_c = rotor speed, rpm
D_b = rotor diameter, in.
L = settling length of rotor, in.
N_m = mixing paddle speed, rpm
D_m = paddle diameter, in.

Although the expression indicates that separating capacity is linearly proportional to the settling length of the rotor, it is obvious that the separating capacity cannot be increased without limit by increasing the rotor length. Increasing the rotor length at any given rotor speed increases the separating capacity, but does not increase pumping capacity proportionately because of the greater lift required. Throughput for a very long rotor would be limited by frictional losses and hydraulic lift requirements.

As can be seen in Fig. 1, the mixed aqueous-organic emulsion flows through the inlet nozzle and is injected into the rotor orifice. The radial vanes quickly accelerate the emulsion to rotor speed, and the phases are separated as they flow up the inside of the rotor. The usual pictorial representation of a high-speed rotor shows a hollow cylindrical air-liquid interface near the axis of the rotor. However, the interface is not truly cylindrical since a small hydraulic head must be developed to overcome the static head from bottom to top and the frictional losses due to fluid flow through the internal passages of the rotor.

Examination of the hydraulic flow conditions can be simplified if one treates the problem first as involving only a single phase. If it is assumed that the rotor is completely filled with fluid, the pressure, p, developed at any radius, r, measured from the axis of the rotor would be

$$p = (1/2)\, \rho \omega^2 r^2 \tag{22}$$

where ρ = fluid density
r = radial distance from axis
ω = rotor speed

By appropriate rearrangement, an equation for hydraulic head, H (measured in feet of any fluid), is obtained in which fluid density, ρ, drops out to give

$$H = \frac{\omega^2 r^2}{2g} \tag{23}$$

where g = force conversion constant, 32.2 (ft)(lb mass)/(lb force)(sec^2), ρ has the unit lb/ft^3, r is in ft, and ω is in radians/sec.

A plot of H vs. r is shown in Fig. 24 for the specific case where ω = 210 radians/sec (2000 rpm). The curve is a parabola of the form $y = Kx^2$. (The horizontal scale is expanded to exaggerate the parabolic form.)

When the rotor operates with an air core along the axis (as it does in centrifugal separating rotors), the net head developed, ΔH, is given by the expression:

$$\Delta H = \frac{\omega^2}{2g} (r_2^2 - r_1^2) \qquad (24)$$

where r_1 = radius of air-liquid surface at the bottom of the rotor
r_2 = radius of air-liquid surface at the overflow point at the top of the rotor

At any given rotor speed, the maximum ΔH is developed in any rotor

when r_1 = radius of the inlet orifice
r_2 = radius of the surface of the fluid flowing over the organic weir.

If two phases are present, some complexities arise because the fluid in the lowest region of the rotor has a variable effective density, depending on the A/O ratio. However, fundamentally, the evaluation is the same as for a single phase. In the contactor shown in Fig. 1, the flow passages for the aqueous phase are at the periphery of the rotor. If there is resistance to aqueous flow through these passages and over the circular weirs, it is automatically balanced by a movement of the aqueous-organic interface (or emulsion band) toward the axis of the rotor. The organic phase flows over the inner weir and rises radially over the weir to a level dependent on its flow rate and the rotor speed. By analogy with rise over a horizontal weir, an equation for calculating rise over a circular weir was developed at Savannah River.[3]

In the series of tests described in Section V, the maximum amount of organic phase that could be pumped through the contactor at 2000 rpm was about 5 gpm. At 5 gpm and 2000 rpm, the rise over the organic weir is 0.109 in. Since the radius of the organic weir is 1.00 in., the radius of the air-organic interface surface is 0.891 in. (0.074 ft). The radius of the rotor orifice is 0.594 in. or 0.050 ft. If Eq. 24 is applied, $\Delta H = (210^2/64.4)(0.074^2 - 0.05^2) = 2$ ft. In Fig. 24, the dotted lines show these two radii and indicate that the ΔH developed between these two points is $\sim$2 ft. The head required to lift organic phase from the inlet orifice to its weir is 1.0 ft. The additional 1 ft of head is consumed in overcoming frictional flow through the rotor and pushing the organic-aqueous emulsion around the edge of the deflection baffle.

At higher rotor speeds, the situation would be essentially the same. A higher net pumping head would be developed, but the increased flow resulting from the increased separating capacity would result in greater frictional losses.

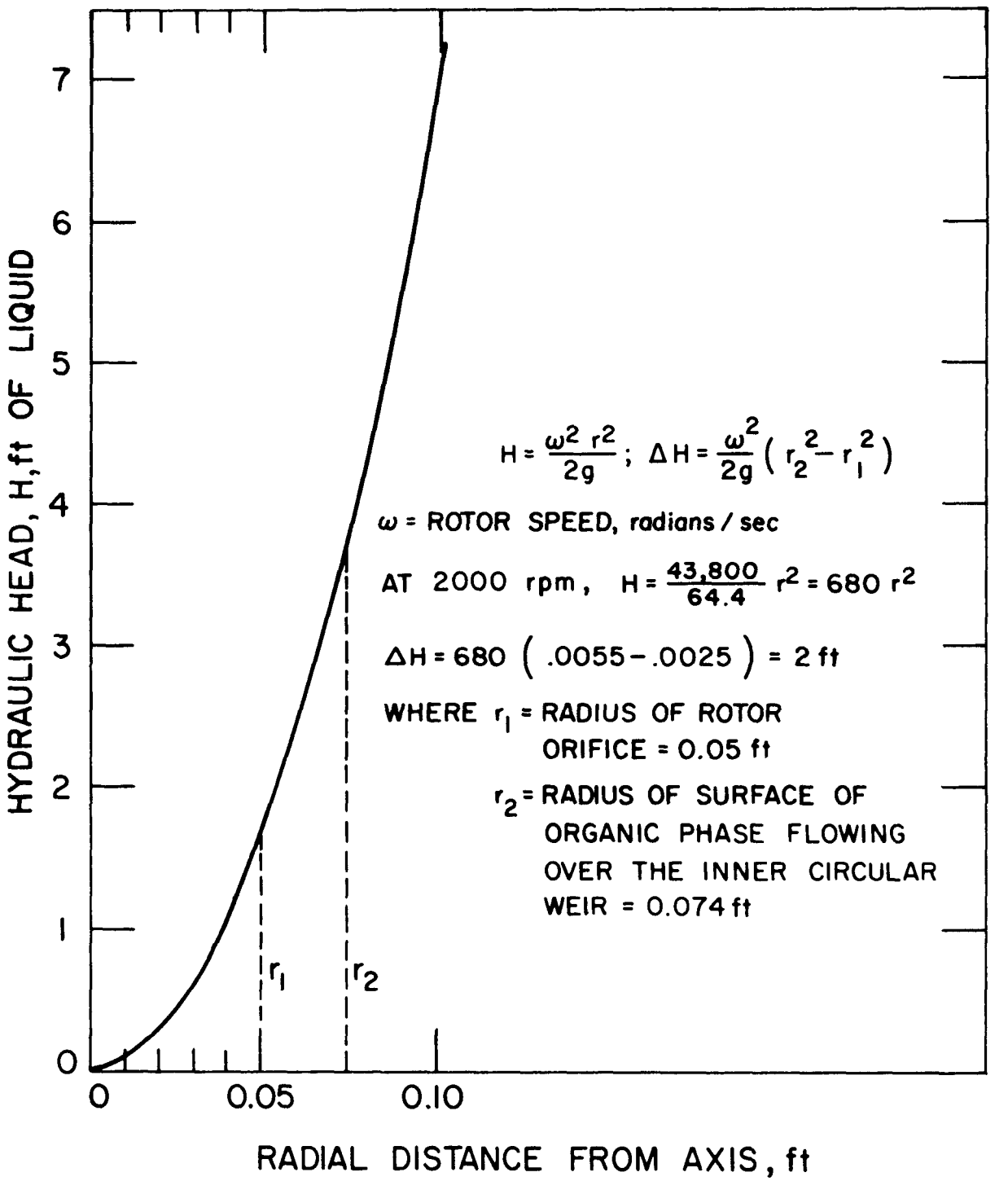

FIG. 24. Hydraulic Head Developed in a Rotor

Although experience with the ANL contactor suggests that the limiting practical L/D ratio is 3, some benefit could still result from using a slightly higher L/D ratio, particularly if some dimensional changes are incorporated in the design. Thus, the inlet orifice could be made slightly smaller and the organic weir could be made slightly larger to increase ΔH. The deflection baffle could be made with a smaller radius since it probably restricts the flow of low-density emulsions around it. In addition, there are some A/O ratios near the 0.5 to 2.0 region where the separating capacity and not the pumping capacity is the flow-limiting factor. It is probable that a rotor designed for use at a more limited range of A/O ratios would show increased separating capacity if its L/D ratio were about 4 or slightly more.

It should be noted that the separating capacity limitations observed in the tests described above are not normally reached in plant operations. In an operating plant, flow rates would be limited to about 70% of the maximum capacity to allow for momentary upsets or perturbations in performance. The flow limitations were observed here because the contactor was operated at the limit of its separating or pumping capacities in the interest of defining the operating characteristics of a contactor having a high L/D.

ACKNOWLEDGMENTS

The authors wish to acknowledge the contributions of N. Quattropani for assistance in the construction and operation of test equipment and the performance of capacity and efficiency tests; of D. S. Webster and A. A. Jonke for overall support and guidance of the program; of H. O. Smith for critical-speed calculations of the rotor and general supervision of overall design drawings; of W. F. Olsen for development of the rotor-speed-indicating device; of A. E. Lissy for radiological monitoring during extraction runs; and of E. Kucera, Z. Tomczuk, and F. Williams for analysis of samples.

REFERENCES

1. E. R. Irish and H. W. Reas, The Purex Process--A Solvent Extraction Reprocessing Method for Irradiated Uranium, USAEC report HW-49483A (April 1957).

2. D. S. Webster, A. S. Jennings, A. A. Kishbaugh, and H. K. Bethmann, Performance of Centrifugal Mixer-Settler in the Reprocessing of Nuclear Fuel, USAEC report DP-MS-67-71 (October 1967).

3. D. S. Webster, C. L. Williamson, and J. F. Ward, Flow Characteristics of a Circular Weir in a Centrifugal Field, USAEC report DP-371 (June 1961).

4. D. S. Webster, C. L. Williamson, and J. F. Ward, Hydraulic Performance of a 5-inch Centrifugal Contactor, USAEC report DP-370 (August 1962).

5. A. T. Clark, Jr., Performance of a 10-inch Centrifugal Contactor, USAEC report DP-752 (September 1962).

6. A. A. Kishbaugh, Performance of a Multi-stage Centrifugal Contactor, USAEC report DP-841 (October 1963).

7. A. S. Jennings, A Miniature Centrifugal Contactor, USAEC report DP-680 (March 1962).

8. G. J. Bernstein, D. E. Grosvenor, J. F. Lenc, and N. M. Levitz, Development and Performance of a High-Speed Annular Centrifugal Contactor, ANL-7969 (to be published).

9. B. F. Roth, Centrifugal Extractors for the Reprocessing of Nuclear Fuels with High Burnup and Plutonium Content, Kernforschungszentrum Karlsruhe, KFK-862 (April 1969).

10. H. K. Clark, Handbook of Nuclear Safety, USAEC report DP-532, Table IV.28, p. 442 (January 1961).

11. R. T. Kent, Mechanical Engineers' Handbook, Design Shop Practice, 11th Ed., John Wiley and Sons, Inc., New York, p. 11-09 (March 1938).

12. M. F. Pushlenkov et al., Study of the Extraction Kinetics of Uranium, Plutonium, Ruthenium, and Zirconium with Tributyl Phosphate with Liquid Mixing in a Centrifugal Field, ORNL-tr-2612 (1971).

13. C. S. Schlea, H. E. Henry, M. R. Caverly, and W. J. Jenkins, Purex Process Performance with Short-Residence Contactors, USAEC report DP-809 (September 1963).

14. O. W. Blodgett, Design of Weldments, The James F. Lincoln Arc Welding Foundation, Cleveland, Ohio, pp. 2.9-7 through 2.9-13 (May 1963).

15. E. R. Maurer and M. O. Withey, Strength of Materials, 2nd Ed., John Wiley and Sons, New York, p. 174 (1935).

16. J. H. Perry, Chemical Engineers' Handbook, 3rd Ed., McGraw-Hill, New York, p. 409 (1950).